DTIC FILE COPY

(2)

AD-A227 259

NAVAL POSTGRADUATE SCHOOL
Monterey, California

THESIS

DTIC ELECTE OCT 09 1990 S E D

COMPUTER AIDED DESIGN MODELS FOR
MILLIMETER-WAVE SUSPENDED
SUBSTRATE MICROSTRIP LINE

by

Choi, Man Soo

March 1990

Thesis Advisor: H. A. Atwater

Approved for public release; distribution is unlimited

90 10 09 022

UNCLASSIFIED

SECURITY CLASSIFICATION OF THIS PAGE

REPORT DOCUMENTATION PAGE

Form Approved OMB No. 0704-0188

1a. REPORT SECURITY CLASSIFICATION UNCLASSIFIED	1b. RESTRICTIVE MARKINGS
2a. SECURITY CLASSIFICATION AUTHORITY	3. DISTRIBUTION/AVAILABILITY OF REPORT Approved for public release; distribution is unlimited
2b. DECLASSIFICATION/DOWNGRADING SCHEDULE	
4. PERFORMING ORGANIZATION REPORT NUMBER(S)	5. MONITORING ORGANIZATION REPORT NUMBER(S)
6a. NAME OF PERFORMING ORGANIZATION Naval Postgraduate School 6b. OFFICE SYMBOL (If applicable) EC	7a. NAME OF MONITORING ORGANIZATION Naval Postgraduate School
6c. ADDRESS (City, State, and ZIP Code) Monterey, CA 93943-5000	7b. ADDRESS (City, State, and ZIP Code) Monterey, CA 93943-5000
8a. NAME OF FUNDING/SPONSORING ORGANIZATION 8b. OFFICE SYMBOL (If applicable)	9. PROCUREMENT INSTRUMENT IDENTIFICATION NUMBER
8c. ADDRESS (City, State, and ZIP Code)	10. SOURCE OF FUNDING NUMBERS PROGRAM ELEMENT NO. / PROJECT NO. / TASK NO. / WORK UNIT ACCESSION NO.

11. TITLE (Include Security Classification) COMPUTER AIDED DESIGN MODELS FOR MILLIMETER-WAVE SUSPENDED SUBSTRATE MICROSTRIP LINE

12. PERSONAL AUTHOR(S)
CHOI, Man Soo

13a. TYPE OF REPORT	13b. TIME COVERED	14. DATE OF REPORT (Year, Month, Day)	15. PAGE COUNT
Master's Thesis	FROM ______ TO ______	1990 March	89

16. SUPPLEMENTARY NOTATION The views expressed in this thesis are those of the author and do not reflect the official policy or position of the Department of Defense or the US Government.

17. COSATI CODES			18. SUBJECT TERMS (Continue on reverse if necessary and identify by block number)
FIELD	GROUP	SUB-GROUP	millimeter wave; suspended substrate; design model

19. ABSTRACT (Continue on reverse if necessary and identify by block number)

An equivalent circuit model was derived for the series gap discontinuity in shielded suspended-substrate transmission line. Numerical values of the circuit parameters were computed for various sets of line dimensions, over a range of operating frequencies.

20. DISTRIBUTION/AVAILABILITY OF ABSTRACT ☒ UNCLASSIFIED/UNLIMITED ☐ SAME AS RPT ☐ DTIC USERS	21. ABSTRACT SECURITY CLASSIFICATION UNCLASSIFIED
22a. NAME OF RESPONSIBLE INDIVIDUAL ATWATER, H.A.	22b. TELEPHONE (Include Area Code) 408-646-3001 22c. OFFICE SYMBOL EC/An

DD Form 1473, JUN 86 Previous editions are obsolete

SECURITY CLASSIFICATION OF THIS PAGE
UNCLASSIFIED

S/N 0102-LF-014-6603

Computer–Aided Design Models for Millimeter–Wave Suspended–Substrate Microstrip Line

by

Choi, Man Soo
Lieutenant, Republic of Korea Navy
B.S., Korean Naval Academy, 1981

Submitted in partial fulfillment of the
requirements for the degree of

MASTER OF SCIENCE IN ELECTRICAL ENGINEERING

from the

NAVAL POSTGRADUATE SCHOOL
March 1990

Author: ______________________
Choi, Man Soo

Approved by: ______________________
H. A. Atwater, Thesis Advisor

____
H. M. Lee, Second Reader

____
John P. Powers, Chairman,
Department of Electrical and Computer Engineering

ABSTRACT

An equivalent circuit model was derived for the series gap discontinuity in shielded suspended-substrate transmission line. Numerical values of the circuit parameters were computed for various sets of line dimensions, over a range of operating frequencies.

TABLE OF CONTENTS

ACKNOWLEDGEMENT

I wish to gratefully express my appreciation to my thesis advisor, Dr. H. A. Atwater, for his invaluable efforts and patience in assisting me through my research. I also want to thank my wife, Young Mi, and my son, Jin Woo, for their support and patience away from our home during two–and–a–half years in the United States.

I. INTRODUCTION

The shielded suspended–substrate line is a transmission medium useful for radar and microwave circuits in the Ka band frequency range, 30 – 40 GHz. In order to utilize this transmission medium in the construction of microwave circuits and filters, it is necessary to have valid circuit models for typical discontinuities such as the series gap in line, open–ended stub, and a discontinuous change in width. These discontinuity characteristics may be deduced on the basis of a calculation of their scattering coefficients for propagating waves in the medium. The approach chosen in this thesis ~~the present work~~, however, is that of placing the selected discontinuity in an open–ended strip resonator in the transmission medium. An appropriate circuit model is adopted for the given discontinuity, and its circuit elements are then deduced on the basis of the perturbation of the resonance frequency of the strip resonator which is induced by the model.

The boundary–value problem associated with the microstrip resonator structure has been approached in a rigorous manner based on a full–wave analysis which utilizes a process of solving the electromagnetic (EM) boundary value problem with inclusion of all the field components. An analysis presented by Itoh and Uwano was employed in the present work [Refs. 1, 3]. (KR)

The characteristic equation for resonant frequencies was obtained by use of Galerkin's technique applied in the spectral or Fourier transform domain. The set of algebraic equations among the transformed quantities thus produced is called the Green's function relations in the transform domain.

II. THEORETICAL ANALYSIS

A. FIELD EQUATIONS

The microstrip resonator to be analyzed is shown in Fig. 1. A rectangular strip of width 2w and length 2ℓ is placed on the suspended substrate. The sides and the top of the structure are surrounded by conducting shield walls. Thus the entire structure is considered to be a suspended-strip resonator located in a partially filled waveguide with end walls.

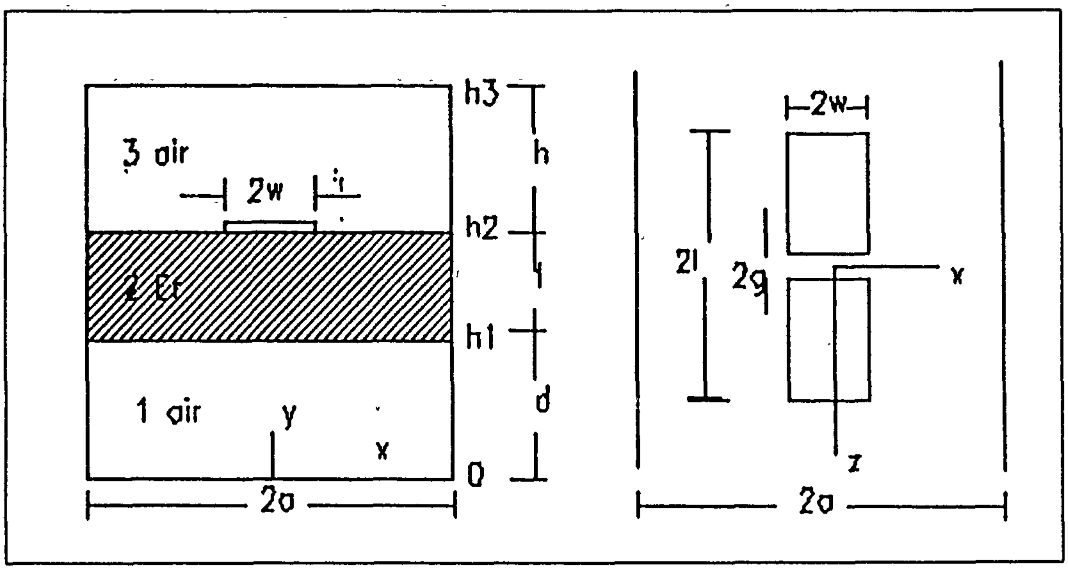

Figure 1. End and top view of Suspended-Substrate Microstrip Line

It is assumed that the thickness of the conducting strip is negligible and that all the media and conductors are lossless. For simplicity, the strip is assumed to be symmetrically located, although the present method of analysis can be easily extended to more general cases.

The fields existing in the structure shown in Fig. 1 are the superposition of TE (to z) and TM (to z) fields, which can be expressed in terms of two types of scalar potentials $\phi^e(x,y,z)$ and $\phi^h(x,y,z)$, where the superscripts e and h denote electric and magnetic, respectively [Ref. 1].

$$E_{zi}(x,y,z) = k_i^2\phi_i^e + \frac{\partial^2\phi_i^e}{\partial z^2} \tag{1a}$$

$$H_{zi}(x,y,z) = k_i^2\phi_i^h + \frac{\partial^2\phi_i^h}{\partial z^2} \tag{1b}$$

$$E_{xi}(x,y,z) = \frac{\partial^2\phi_i^e}{\partial x\partial z} - j\omega\mu_i\frac{\partial\phi_i^h}{\partial y} \tag{1c}$$

$$H_{xi}(x,y,z) = \frac{\partial^2\phi_i^h}{\partial x\partial z} + j\omega\epsilon_i\frac{\partial\phi_i^e}{\partial y} \tag{1d}$$

where i = 1, 2, 3 designates the substrate or the air region, as shown in Fig. 1.

$$k_1^2 = k_3^2 = k_0^2 = \mu_0\epsilon_0\omega^2 \tag{1e}$$

$$k_2^2 = \mu_2\epsilon_2\omega^2 = \mu_r\epsilon_r k_0^2 \tag{1f}$$

$$\epsilon_1 = \epsilon_3 = \epsilon_0 \tag{1g}$$

$$\epsilon_2 = \epsilon_r\epsilon_0 \tag{1h}$$

$$\mu_1 = \mu_3 = \mu_0 \tag{1i}$$

$$\mu_2 = \mu_r\mu_0 = \mu_0, \quad (\mu_r = 1) \tag{1j}$$

where ω is the operating frequency and ϵ_0 and μ_0 are the free-space permittivity and permeability.

B. BOUNDARY CONDITIONS

Now applying boundary conditions at the bottom in region 1, tangential electric field and normal magnetic field components must be zero.

$$E_{z1}(x,0,z) = 0, \quad \frac{\partial}{\partial y} H_{z1}(x,0,z) = 0 \tag{2a}$$

$$E_{x1}(x,0,z) = 0, \quad \frac{\partial}{\partial y} H_{x1}(x,0,z) = 0 \tag{2b}$$

At the interface between regions 1 and 2, the tangential field components must be continuous.

At $y = h_1$:

$$E_{z1}(x,h_1,z) = E_{z2}(x,h_1,z) \tag{3a}$$

$$E_{x1}(x,h_1,z) = E_{x2}(x,h_1,z) \tag{3b}$$

$$H_{z1}(x,h_1,z) = H_{z2}(x,h_1,z) \tag{3c}$$

$$H_{x1}(x,h_1,z) = H_{x2}(x,h_1,z) \tag{3d}$$

At the interface between regions 2 and 3, tangential electric field components must be continuous.

At $y = h_2$:

$$E_{z2}(x,h_2,z) = E_{z3}(x,h_2,z) \tag{4a}$$

$$E_{x2}(x,h_2,z) = E_{x3}(x,h_2,z) \tag{4b}$$

Also, the electric fields at $y = h_2$ will exist only on the air/dielectric interface, and can be expressed as,

$$E_{z2}(x,h_2,z) = \begin{cases} E_z(x)e^{\gamma z}, & a > |x| \geq w, \\ 0 \ , & \text{otherwise} \end{cases} \tag{4c}$$

$$E_{x3}(x,h_2,z) = \begin{cases} E_x(x)e^{\gamma z}, & a > |x| \geq w, \\ 0 \ , & \text{otherwise} \end{cases} \tag{4d}$$

Similarly, tangential magnetic fields at h_2 must be discontinuous by the corresponding surface current densities.

$$H_{z2}(x,h_2,z) - H_{z3}(x,h_2,z) = \begin{cases} J_x(x)e^{\gamma z}, & |x| \leq w, \\ 0, & \text{otherwise} \end{cases} \tag{4e}$$

$$H_{x2}(x,h_2,z) - H_{x3}(x,h_2,z) = \begin{cases} J_z(x)e^{\gamma z}, & |x| \leq w, \\ 0, & \text{otherwise} \end{cases} \tag{4f}$$

At the top in region 3. tangential E–field components must be zero.

At $y = h_3$:

$$E_{z3}(x,h_3,z) = 0, \qquad \frac{\partial H_{z3}}{\partial y}(x,h_3,z) = 0 \tag{5a}$$

$$E_{x3}(x,h_3,z) = 0, \qquad \frac{\partial H_{x3}}{\partial y}(x,h_3,z) = 0 \tag{5b}$$

The final boundary conditions occur at $x = \pm \frac{a}{2}$ where the tangential E–field components must be zero in all regions.

At $x = \pm\frac{a}{2}$:

$$E_{zi}(\pm\frac{a}{2},y,z) = 0 \tag{6a}$$

$$E_{yi}(\pm\frac{a}{2},y,z) = 0 \tag{6b}$$

C. SPECTRAL DOMAIN APPROACH.

The boundary value problem is solved in the Fourier transform or spectral domain. This leads to the Green's function equations associated with the structure. This analysis was first carried out by Itoh and Mittra and was successfully applied to a number of problems in microwave integrated circuit structures [Ref. 7].

1. Potential Equations

The quantities in Eqs. (1) are transformed into spectral domain via the Fourier transform;

$$\tilde{\phi}_i^{e,h}(n,y,\beta) = \int_{-\infty}^{\infty} dz \int_{-a}^{a} dx \tilde{\phi}_i^{e,h}(x,y,z) e^{jk_n x} e^{j\beta z} \qquad n = 1, 2, \cdots \tag{7a}$$

where β is the Fourier transform variable, k_n is the discrete transform variable defined by,

$$k_n = \frac{(n - \frac{1}{2})\pi}{a} \text{ for } E_z \text{ even, } -H_z \text{ odd(in x) modes.} \tag{7b}$$

$$k_n = \frac{n \cdot \pi}{a} \text{ for } E_z \text{ odd, } -H_z \text{ even(in x) modes.} \tag{7c}$$

The transforms of field quantities are now,

$$\tilde{E}_{zi}(n,y,\beta) = k_{ci}^2 \tilde{\phi}_i^e \tag{8a}$$

$$\tilde{H}_{zi}(n,y,\beta) = k_{ci}^2 \tilde{\phi}_i^h \tag{8b}$$

$$\tilde{E}_{xi}(n,y,\beta) = -k_n \beta \tilde{\phi}_i^e - j\omega\mu_i \frac{\partial \tilde{\phi}_i^h}{\partial y} \tag{8c}$$

$$\tilde{H}_{xi}(n,y,\beta) = -k_n \beta \tilde{\phi}_i^h + j\omega\epsilon_i \frac{\partial \tilde{\phi}_i^e}{\partial y} \tag{8d}$$

$$k_{ci}^2 = k_i^2 + \Gamma^2, \; (\Gamma = -j\beta, \; k_i^2 = \omega^2 \mu_i \epsilon_i) \tag{8e}$$

$$k_{ci}^2 = k_i^2 - \beta^2 = \mu_0 \epsilon_0 \epsilon_{r_i} \omega^2 - \beta^2 \tag{8f}$$

where i = 1, 2, 3, for each of the three regions defined in Fig. 1.

The transforms of scalar potentials satisfy,

$$\frac{d^2\tilde{\phi}_i^{e,h}}{dy^2} - \gamma_i^2\tilde{\phi}_i^{e,h} = 0 \tag{9a}$$

where $\gamma_i^2 = k_n^2 - k_{ci}^2 \begin{cases} \gamma_1^2 = \gamma_3^2 = k_n^2 - k_{c1,3}^2 = k_n^2 + \beta^2 - k_0^2 \\ \gamma_2^2 = k_n^2 - k_{c2}^2 = k_n^2 + \beta^2 - \epsilon_r\mu_r k_0^2 \end{cases}$

The solutions for these homogeneous differential equations are well known and can be described in the general form as below,

$$\tilde{\phi}_i = C_1\cosh\gamma y + C_2\sinh\gamma y. \tag{9b}$$

Now the boundary conditions (2), and (5) are applied. The cosh term vanishes in electric field and the sinh term vanishes in magnetic field in regions 1 and 3. The potentials are: (see details in Appendix A),

Region (1)

$$\tilde{\phi}_1^e = A\sinh\gamma_1 y \tag{10a}$$

$$\tilde{\phi}_1^h = B\cosh\gamma_1 y \tag{10b}$$

Region (2)

$$\tilde{\phi}_2^e = C\sinh\gamma_2 y + D\cosh\gamma_2 y \tag{10c}$$

$$\tilde{\phi}_2^h = E\sinh\gamma_2 y + F\cosh\gamma_2 y \tag{10d}$$

Region (3)

$$\tilde{\phi}_3^e = G\sinh\gamma_3(y - h_3) \tag{10e}$$

$$\tilde{\phi}_3^h = H\cosh\gamma_3(y - h_3) \tag{10f}$$

where

$$\gamma_i^2 = k_n^2 - k_{ci}^2 = k_n^2 + \beta^2 - k_i^2 \tag{10g}$$

$$k_n = \begin{cases} \dfrac{n\pi}{a}, & \tilde{\phi}^h \text{ even} \\ \dfrac{(n - \frac{1}{2})\pi}{a}, & \tilde{\phi}^h \text{ odd} \end{cases} \tag{10h}$$

2. Green's Function

In conventional space domain analysis, the structure may be analyzed by first formulating the following coupled homogeneous integral equations. The equations must then be solved for the unknown propagation constant β.

$$\int [Z_{zz}(x-x',y)J_z(x') + Z_{zx}(x-x',y)J_x(x')]dx' = E_z(x) \tag{11a}$$

$$\int [Z_{xz}(x-x',y)J_z(x') + Z_{xx}(x-x',y)J_x(x')]dx' = E_x(x) \tag{11b}$$

where E_z and E_x are unknown electric fields on the boundary at $y = h_2$, J_z and J_x are current components on the strip at $y = h_2$, and the Green's functions $Z_{i,j}(i,j = z,x)$ are functions of β.

The integration is over the strip where $E_z(x)$ and $E_x(x)$ are zero, as the strip is assumed to be perfectly conducting. In the spectral domain formulation, however, the following algebraic equations, instead of the coupled integral equations, are obtained. These equations are the Fourier transform equivalent of the coupled integral equations.

$$\tilde{Z}_{zz}(k_n,h_2)\tilde{J}_z(k_n) + \tilde{Z}_{zx}(k_n,h_2)\tilde{J}_x(k_n) = \tilde{E}_z(k_n,h_2) \tag{12a}$$

$$\tilde{Z}_{xz}(k_n,h_2)\tilde{J}_z(k_n) + \tilde{Z}_{xx}(k_n,h_2)\tilde{J}_x(k_n) = \tilde{E}_x(k_n,h_2) \tag{12b}$$

where quantities with tildes (~) are Fourier transforms of corresponding quantities. The Fourier transform is defined as in Eq. (7).

The right-hand side of equations (12) is not zero everywhere because the Fourier transform requires integration over all x, not only over the strip. The equations contain four unknowns J_z, J_x, E_z, and E_x, with unknown β. However, E_z and E_x will be eliminated in the solution process based on the Galerkin procedure.

In the spectral domain, the boundary conditions (3), (4) are now given by the following equations.

at $y = h_1$,

$$\tilde{E}_{z1} = \tilde{E}_{z2}$$

$$\tilde{E}_{x1} = \tilde{E}_{x2}$$

$$\tilde{H}_{z1} = \tilde{H}_{z2}$$

$$\tilde{H}_{x1} = \tilde{H}_{x2}$$

at $y = h_2$,

$$\tilde{E}_{z2} = \tilde{E}_{z3}$$

$$\tilde{E}_{x2} = \tilde{E}_{x3}$$

$$\tilde{H}_{z2} - \tilde{H}_{z3} = -\tilde{J}_x$$

$$\tilde{H}_{x2} - \tilde{H}_{x3} = \tilde{J}_z$$

where $\tilde{J}_z$ and $\tilde{J}_x$ are Fourier transforms of unknown current components $J_z(x)$ and $J_x(x)$ on the strip at $y = h_2$.

When the fields are expressed in terms of the potentials, these can be put into the form: [Ref. 3]

$$\begin{bmatrix}\tilde{E}_z\\ \tilde{E}_x\end{bmatrix} = \begin{bmatrix}\tilde{Z}_{zz} & \tilde{Z}_{zx}\\ \tilde{Z}_{xz} & \tilde{Z}_{xx}\end{bmatrix}\begin{bmatrix}\tilde{J}_z\\ \tilde{J}_x\end{bmatrix} \tag{13}$$

where

$$\tilde{Z}_{zz} = -\frac{1}{k_n{}^2+\beta^2}[\beta^2\tilde{Z}_e + k_n{}^2\tilde{Z}_h]$$

$$\tilde{Z}_{xz} = \tilde{Z}_{zx} = -\frac{k_n\beta}{k_n{}^2+\beta^2}[\tilde{Z}_e - \tilde{Z}_h]$$

$$\tilde{Z}_{xx} = -\frac{1}{k_n{}^2+\beta^2}[k_n{}^2\tilde{Z}_e + \beta^2\tilde{Z}_h]$$

$$\tilde{Z}_e = \frac{\gamma_{y2}Ct_1 + \gamma_{y1}Ct_2}{Ct_1Ct_2 + Ct_1Ct_3\frac{\gamma_{y2}}{\gamma_{y3}} + Ct_2Ct_3\frac{\gamma_{y1}}{\gamma_{y3}} + \frac{\gamma_{y1}}{\gamma_{y2}}}$$

$$\tilde{Z}_h = \frac{\gamma_{z2}Ct_2 + \gamma_{z1}Ct_1}{\gamma_{z1}\gamma_{z2}Ct_1Ct_2 + \gamma_{z1}\gamma_{z3}Ct_1Ct_3 + \gamma_{z2}\gamma_{z3}Ct_2Ct_3 + \gamma_{z2}^2}$$

For $\gamma_i \geq 0$

$$Ct_1 = \coth\gamma_1 d, \quad Ct_2 = \coth\gamma_2 t, \quad Ct_3 = \coth\gamma_3 h,$$

For $\gamma_i < 0$

$$Ct_1 = -j\cot\gamma_1 d, \quad Ct_2 = -j\cot\gamma_2 t, \quad Ct_3 = -j\cot\gamma_3 h,$$

$$\gamma_i = \sqrt{k_n{}^2 + \beta^2 - \mu_0\epsilon_i\omega^2}$$

$$\gamma_{yi} = \frac{\gamma_i}{j\omega\epsilon_i}, \quad \gamma_{zi} = \frac{\gamma_i}{j\omega\mu_i}.$$

The quantities $\tilde{Z}_{zz}$, $\tilde{Z}_{zx}$, $\tilde{Z}_{xz}$ and $\tilde{Z}_{xx}$ are actually the Fourier transforms of dyadic Green's function components.

3. Characteristic Equations in Matrix Form

Two equations in (13) contain four unknowns $\tilde{E}_z$, $\tilde{E}_x$, $\tilde{J}_z$ and $\tilde{J}_x$. However, the first two unknowns $\tilde{E}_z$ and $\tilde{E}_x$ can be eliminated by applying Galerkin's method in the spectral domain. The first step is to expand the unknown $\tilde{J}_z$ and $\tilde{J}_x$ in terms of assumed basis functions $\tilde{J}_{zm}$ and $\tilde{J}_{xm}$ with unknown coefficients c_m and d_m.

$$\tilde{J}_z(n,\beta) = \sum_{m=1}^{N} c_m \tilde{J}_{zm}(n,\beta) \tag{14a}$$

$$\tilde{J}_x(n,\beta) = \sum_{m=1}^{M} d_m \tilde{J}_{xm}(n,\beta) \tag{14b}$$

The basis functions $\tilde{J}_{zm}$ and $\tilde{J}_{xm}$ must be chosen to be the Fourier transforms of space-domain functions $J_{zm}(x,z)$ and $J_{xm}(x,z)$ which are physically realistic, and which are zero except for the region $|x| < w$ and $|z| < \ell$. Now, substituting (14) into (13) and taking inner products of the resulting equations with the basis function $\tilde{J}_{zi}$ and $\tilde{J}_{xi}$ for different values of i yields the matrix equation,

$$\int [\tilde{J}_{zi}\tilde{Z}_{zz} \sum_{m=1}^{N} c_m \tilde{J}_{zm} + \tilde{J}_{zi}\tilde{Z}_{zx} \sum_{m=1}^{M} d_m \tilde{J}_{xm}] d\beta = 0, \tag{15a}$$

$$i = 1, 2, \cdots\cdots\cdots, M.$$

$$\int [\tilde{J}_{xi}\tilde{Z}_{xz} \sum_{m=1}^{N} c_m \tilde{J}_{zm} + \tilde{J}_{xi}\tilde{Z}_{xx} \sum_{m=1}^{M} d_m \tilde{J}_{xm}] d\beta = 0, \tag{15b}$$

$$i = 1, 2, \cdots\cdots\cdots, N.$$

The right-hand sides of (15) are zero by virtue of Parseval's theorem, because the currents $J_{zi}(x)$, $J_{xi}(x)$ and the field components $E_z(x,h_2)$, $E_x(x,h_2)$ vanish in complementary regions of x. For example, if the inner product of $\tilde{E}_z$ on the left-hand side of (13) with $\tilde{J}_{zi}(k_n)$ is taken, one obtains

$$\int_{-\infty}^{\infty} \tilde{J}_{zi}(k_n)\tilde{E}_z(k_n)dk_n = 2\pi \int_{-\infty}^{\infty} J_{zi}(x)E_{zi}(x)dx = 0$$

In the above, $J_{zi}(x)$ is zero outside the strip, and $E_z(x)$ is zero on the strip.

Therefore, the final boundary condition is now used.

Equations (15) will be expressed in matrix form as follows,

$$\sum_{m=1}^{N} K_{im}^{(1,1)} c_m + \sum_{m=1}^{M} K_{im}^{(1,2)} d_m = 0, \qquad i = 1, 2, \cdots, N. \tag{16a}$$

$$\sum_{m=1}^{N} K_{im}^{(2,1)} c_m + \sum_{m=1}^{M} K_{im}^{(2,2)} d_m = 0, \qquad i = 1, 2, \cdots, M. \tag{16b}$$

where from the definition of the inner products associated with the Fourier transform defined by (7), the matrix elements are

$$K_{im}^{(1,1)}(k_0) = \sum_{n=1}^{\infty} \int_0^{\infty} \tilde{J}_{zi}(n,\beta)\tilde{Z}_{zz}\tilde{J}_{zm}(n,\beta)d\beta \tag{17a}$$

$$K_{im}^{(1,2)}(k_0) = \sum_{n=1}^{\infty} \int_0^{\infty} \tilde{J}_{zi}(n,\beta)\tilde{Z}_{zx}\tilde{J}_{xm}(n,\beta)d\beta \tag{17b}$$

$$K_{im}^{(2,1)}(k_0) = \sum_{n=1}^{\infty} \int_0^{\infty} \tilde{J}_{xi}(n,\beta)\tilde{Z}_{xz}\tilde{J}_{zm}(n,\beta)d\beta \tag{17c}$$

$$K_{im}^{(2,2)}(k_0) = \sum_{n=1}^{\infty} \int_0^{\infty} \tilde{J}_{xi}(n,\beta)\tilde{Z}_{xx}\tilde{J}_{xm}(n,\beta)d\beta \tag{17d}$$

A homogeneous system of equations is thus obtained in terms of the unknown coefficients c_m and d_m. In order that c_m and d_m have nontrivial solutions, the determinant of the matrix must be zero, and hence the resonant frequency ω is determined for the resonator and discontinuity assumed.

Equations (16) are now solved for the wave number k_0 by setting the determinant of the coefficient matrix equal to zero and by seeking the root of the resulting characteristic equation. The resonance frequency of the suspended-stripline resonator is derived from the obtained value of k_0.

The accuracy of the solution can be systematically improved by increasing the number of basis functions (M+N) and by solving larger size matrix equations. However, if the first few basis functions are chosen so as to

approximate the actual unknown current distribution reasonably well, the necessary size of the matrix can be held small for a given accuracy of the solution, resulting in numerical efficiency. Hence the choice of basis functions is important from the numerical point of view.

$$J_{z1}(z) = b \tag{20a}$$

$$J_{z2}(z) = \begin{cases} -\frac{1}{2\ell_1}\sin(\frac{\pi z}{\ell_1} + \frac{g\pi}{\ell_1}), & -p_2 \le z \le -g,\ \ell_1 = p_2 - g \\ \frac{1}{2\ell_2}\sin(\frac{\pi z}{\ell_2} - \frac{g\pi}{\ell_2}), & g \le z \le p_1,\ \ell_2 = p_1 - g \end{cases} \tag{20b}$$

With a gap present assume $J_x = 0$, and $J_z = c_1 J_{z1} + c_2 J_{z2}$, with distributions as shown in Fig. 3. The transformed distributions are:

$$\tilde{J}_{z1} = \tilde{J}_{z1}(\beta)\cdot\tilde{J}_{zx}(k_n) \tag{21a}$$

$$\tilde{J}_{z2} = \tilde{J}_{z2}(\beta)\cdot\tilde{J}_{zx}(k_n) \tag{21b}$$

$\tilde{J}_{zx}(k_n)$ is same as in Fig. 2.

$$\tilde{J}_{z1}(\beta) = -j\frac{e^{j\beta p_1} - e^{-j\beta p_2} - 2j\sin(\beta g)}{\beta(p_1 + p_2 - 2g)} \tag{22a}$$

$\tilde{J}_{z2}(\beta) =$

$$\frac{1}{4}\left\{e^{j\frac{g\pi}{d_2}}\frac{e^{-j(\frac{\pi}{d_2}+\beta)g} - e^{-j(\frac{\pi}{d_2}+\beta)p_2}}{\pi + \beta d_1} + e^{-j\frac{g\pi}{d_2}}\frac{e^{j(\frac{\pi}{d_2}-\beta)g} - e^{j(\frac{\pi}{d_2}-\beta)p_2}}{\pi - \beta p_2}\right.$$

$$\left. - e^{-j\frac{g\pi}{d_1}}\frac{e^{j(\frac{\pi}{d_1}+\beta)p_1} - e^{j(\frac{\pi}{d_1}+\beta)g}}{\pi + \beta d_1} - e^{j\frac{g\pi}{d_1}}\frac{e^{-j(\frac{\pi}{d_1}-\beta)p_1} - e^{-j(\frac{\pi}{d_1}-\beta)g}}{\pi - \beta d_1}\right\} \tag{22b}$$

From Eq. (15a) and with i = 1,

$$\tilde{J}_{zi}\tilde{Z}_{zz}c_m\tilde{J}_{zm} = \tilde{J}_{z1}(n,\beta)\tilde{Z}_{zz}c_1\tilde{J}_{z1} + \tilde{J}_{z1}(n,\beta)\tilde{Z}_{zz}c_2\tilde{J}_{z2} \tag{23a}$$

and, with i = 2, this takes the form

$$\tilde{J}_{zi}\tilde{Z}_{zz}c_m\tilde{J}_{zm} = \tilde{J}_{z2}(n,\beta)\tilde{Z}_{zz}c_1\tilde{J}_{z1} + \tilde{J}_{z2}(n,\beta)\tilde{Z}_{zz}c_2\tilde{J}_{z2} \tag{23b}$$

These equations can be represented in the matrix form:

$$\begin{bmatrix} K11 & K12 \\ K21 & K22 \end{bmatrix}\begin{bmatrix} c_1 \\ c_2 \end{bmatrix} = \begin{bmatrix} 0 \\ 0 \end{bmatrix} \tag{24}$$

where,

$$K11 = \Sigma\int \tilde{J}_{z1}(n,\beta)\tilde{Z}_{zz}\tilde{J}_{z1}(n,\beta)d\beta \qquad K12 = \Sigma\int \tilde{J}_{z1}(n,\beta)\tilde{Z}_{zz}\tilde{J}_{z2}(n,\beta)d\beta$$

$$K21 = \Sigma\int \tilde{J}_{z2}(n,\beta)\tilde{Z}_{zz}\tilde{J}_{z1}(n,\beta)d\beta \qquad K22 = \Sigma\int \tilde{J}_{z2}(n,\beta)\tilde{Z}_{zz}\tilde{J}_{z2}(n,\beta)d\beta$$

B. BOUNDARY VALUES

The actual computation was carried out using the shield and line dimensions shown in column 1, in Table 1, which is typical data from a suspended stripline filter problem initiated by the NOSC (Naval Ocean Systems Center) Microwave Laboratory in San Diego. This configuration is used in the frequency range of 30 – 40 GHz.

The data in columns 2 and 3 were used in analysis of the microstrip line with a gap, to compare with published data [Ref 5].

Data 2 uses frequency range of 85 – 102 GHz

Data 3 uses frequency range of 31 – 40 GHz

TABLE 1. CONFIGURATION DATA

(dimensions : mm)

Data	1	2	3
a	3.2	1.27	3.56
d	0.6604	0.318	0.763
t	0.254	0.127	0.127
h	0.6604	0.19	0.89
w	0.7112	0.6	1.5
g	0.26452	0.1 – 0.6	0.2 – 1.6
Er	2.2	2.22	2.22

Symbols for Fig. 1

a = Shield width

d = Height of lower air layer

t = Height of dielectric substrate layer

h = Height of upper air layer

w = Microstrip line width

g = Gap in microstrip line(center)

Er = dielectric constant of substrate layer.

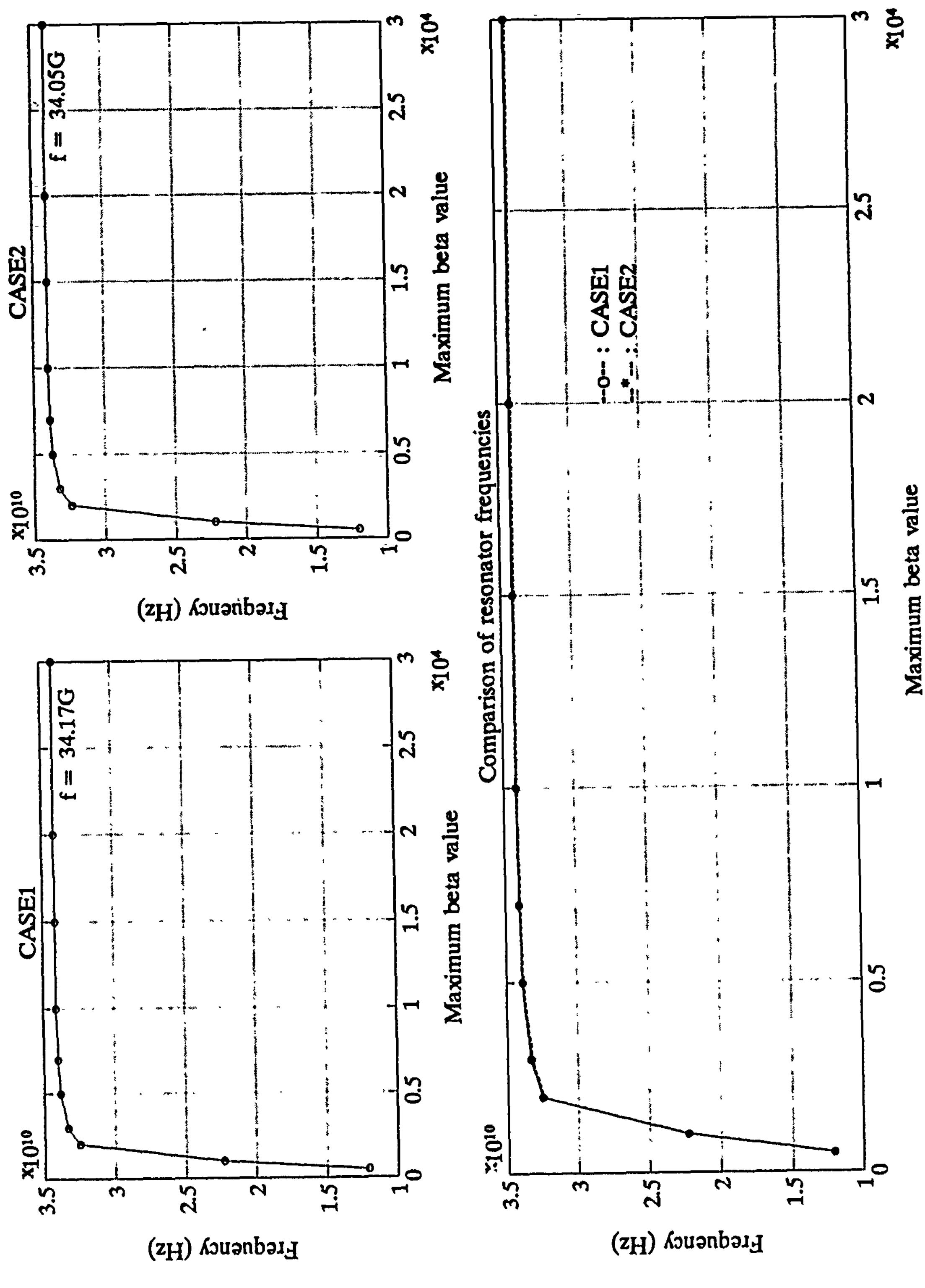

Figure 4. Resonator frequencies of strip without gap, vs. upper limit(β_{max}) of Fourier integral.

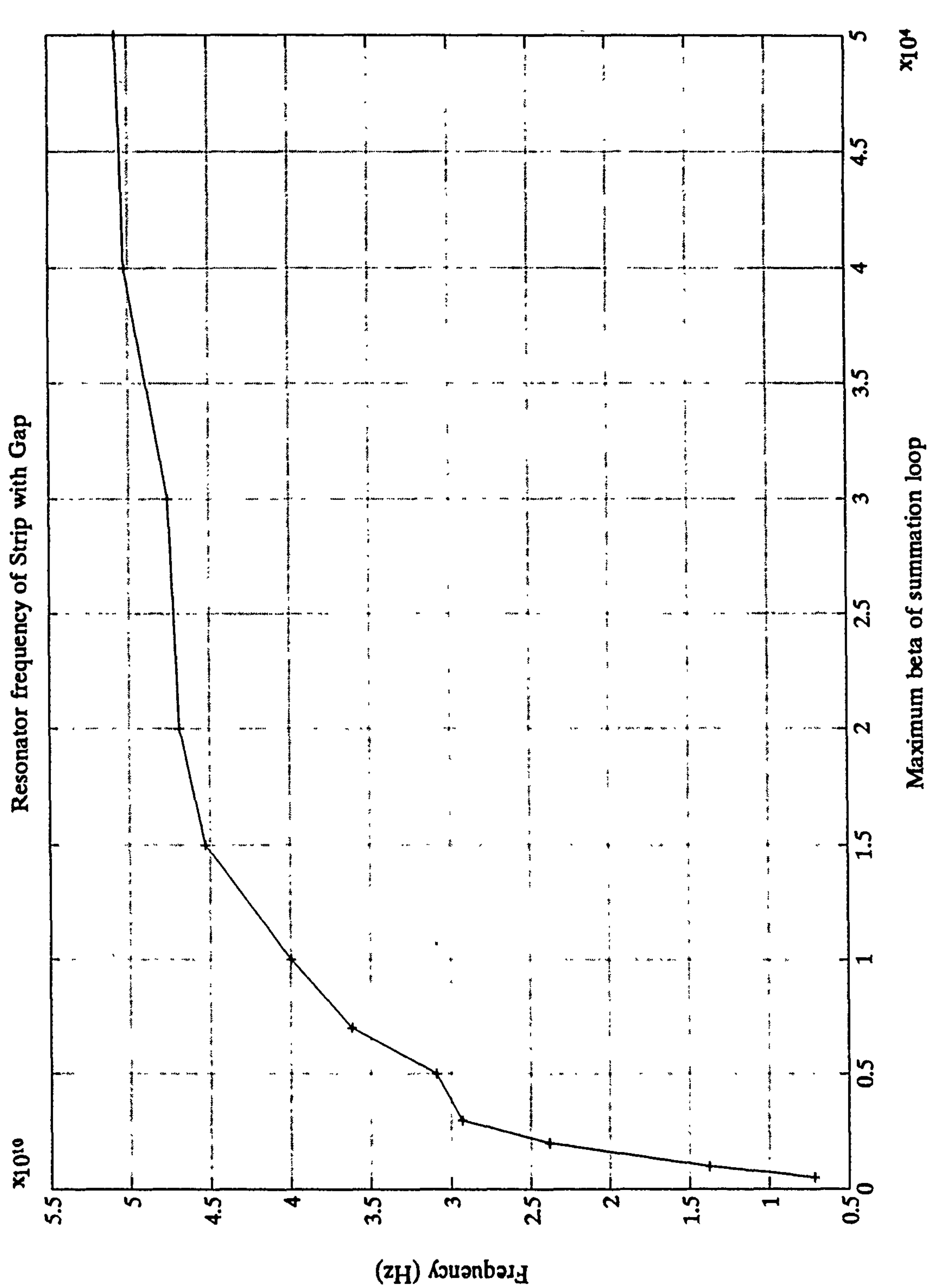

Figure 5. Resonator frequency of strip including gap

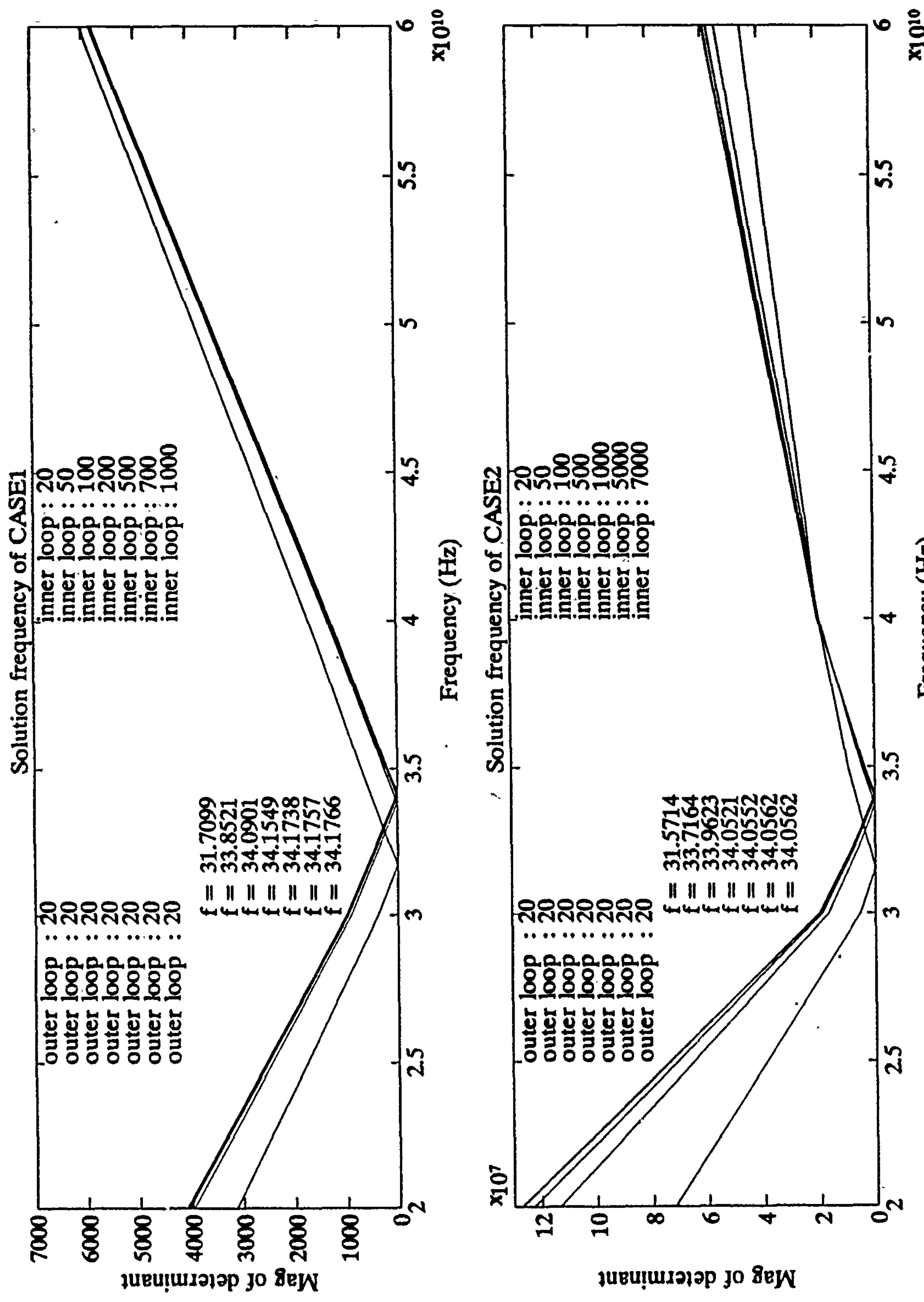

Figure 7. Solution frequencies for the determinant

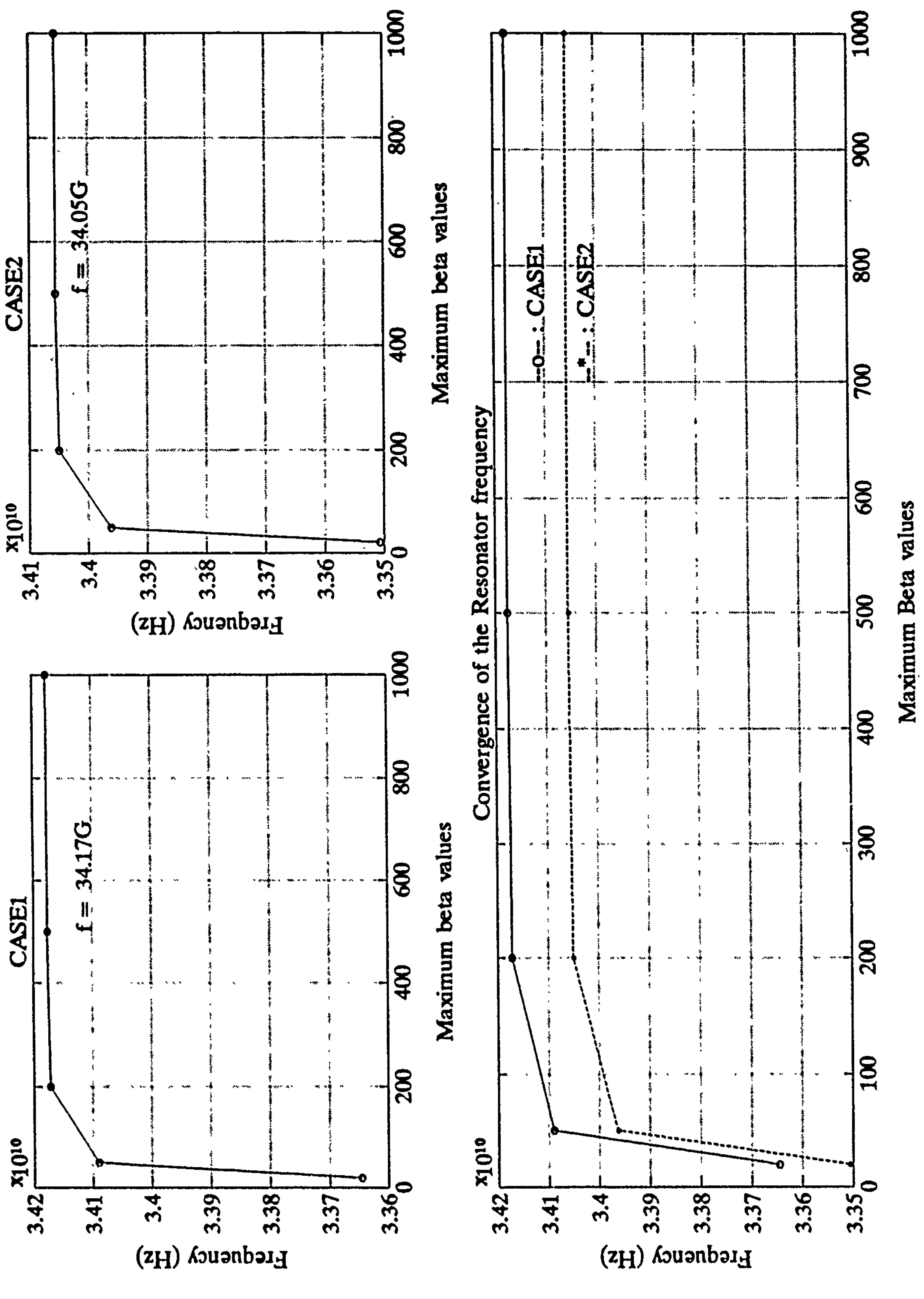

Figure 8. Result of double summation

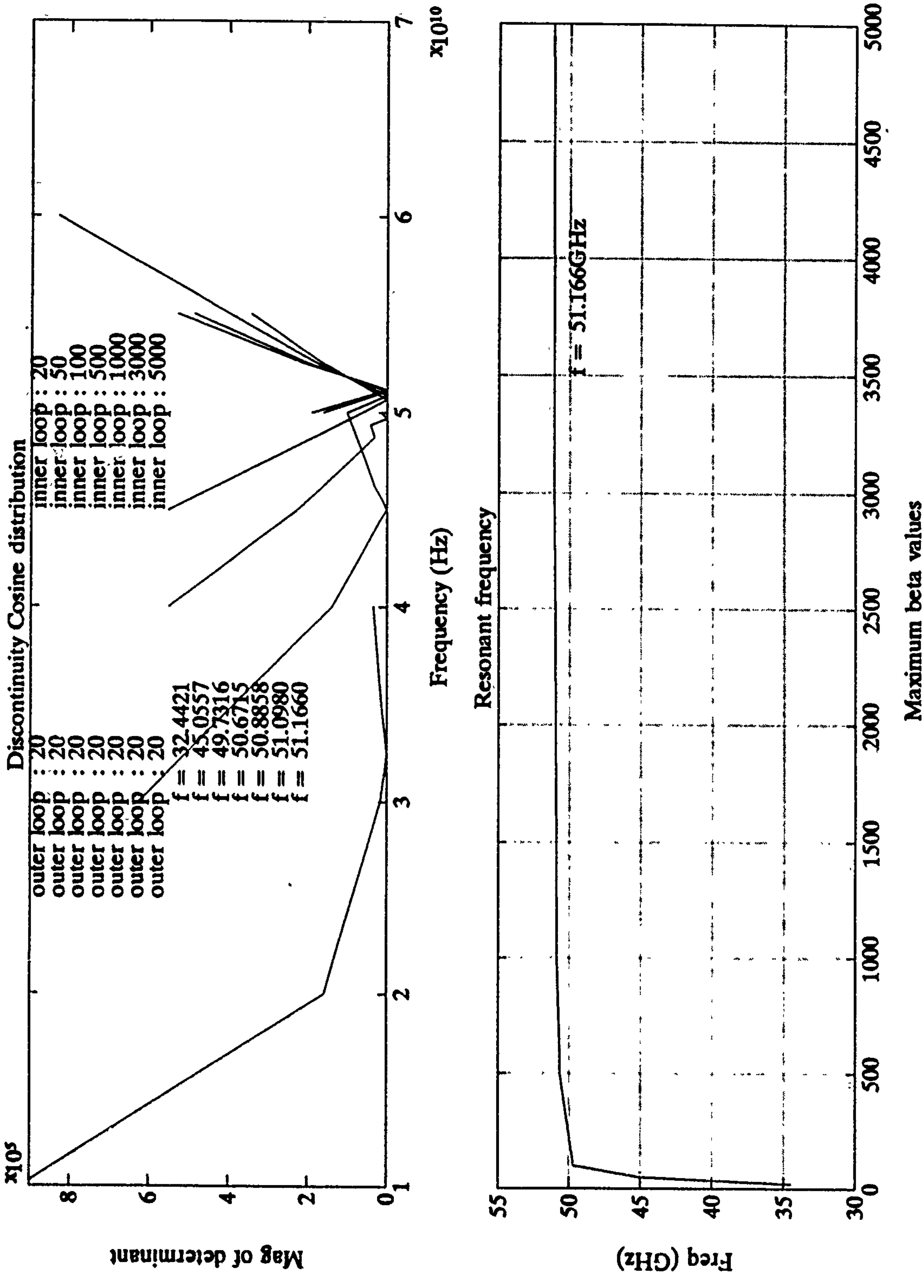

Figure 9. Resonator and gap solution with double summation

4. Analysis of Resonator with Gap Present

a. Resonance stub lengths at given frequency pairs

The moment method calculation (Appendix D. part A) was carried out with various assumed stub lengths. The results are shown in Table 2 and Table 3.

TABLE 2. RESONATOR STUB LENGTHS WITH DATA 2 (SEC. III-B)

Units
length : mm
frequency : GHz

g/2 \ f	86(85)	94(93)	102(101)
0.05	1.211647 (1.230606)	1.075264 (1.090897)	0.959969 (0.973572)
0.1	1.259331 (1.278259)	1.121864 (1.137848)	1.005066 (1.014435)
0.15	1.285843 (1.304749)	1.147675 (1.163574)	1.030686 (1.044349)
0.2	1.300917 (1.319977)	1.163193 (1.179146)	1.045738 (1.059464)
0.25	1.310349 (1.329392)	1.172264 (1.188179)	1.055008 (1.068817)
0.3	1.316086 (1.334999)	1.178024 (1.193985)	1.060890 (1.074570)

c. Effective dielectric constant

The calculation of the effective dielectric constant used the β values which were computed above (Table 4).

$$\beta = \frac{\omega}{c}\cdot\sqrt{\epsilon_{eff}}$$

$$\epsilon_{eff} = \left[\frac{\beta c}{\omega}\right]^2$$

d. Characteristic impedance Z_0 [Ref. 6]

The computation of characteristic impedance uses an empirical calculation for the quasistatic value, $Z_0(0)$ [Ref. 5] which has been confirmed to be accurate [Ref. 8]. This value is then corrected to the wanted frequency f by use of $\epsilon_{eff}(f)$ in the expression:

$$Z_0(f) = \frac{Z_0(0)}{\sqrt{\epsilon_{eff}}} \qquad \text{(Appendix D. part B. data file)}$$

(1) for $0 < w < \frac{a}{2}$;

$$Z_1 = 60\left[V + R\cdot \ln\left\{6\frac{b}{w} + \sqrt{1 + 4(\frac{b}{w})^2}\right\}\right]$$

$$Z_0 = \frac{Z_1}{\sqrt{\epsilon_{eff}}}$$

$$V = -1.7866 - 0.2035(\frac{h}{b}) + 0.4750(\frac{a}{b})$$

$$R = 1.0835 + 0.1007(\frac{h}{b}) - 0.09457(\frac{a}{b})$$

(2) when $\frac{a}{2} < w < a$;

$$Z_1 = 120\pi[V + R\{\frac{w}{b} + 1.3930 + 0.6670\cdot \ln(\frac{w}{b} + 1.444)\}^{-1}]$$

$$Z_0 = \frac{Z_1}{\sqrt{\epsilon_{eff}}}$$

$$V = -0.6301 - 0.07082(\frac{h}{b}) + 0.2470(\frac{a}{b})$$

$$R = 1.9492 + 0.1553(\frac{h}{b}) - 0.5123(\frac{a}{b})$$

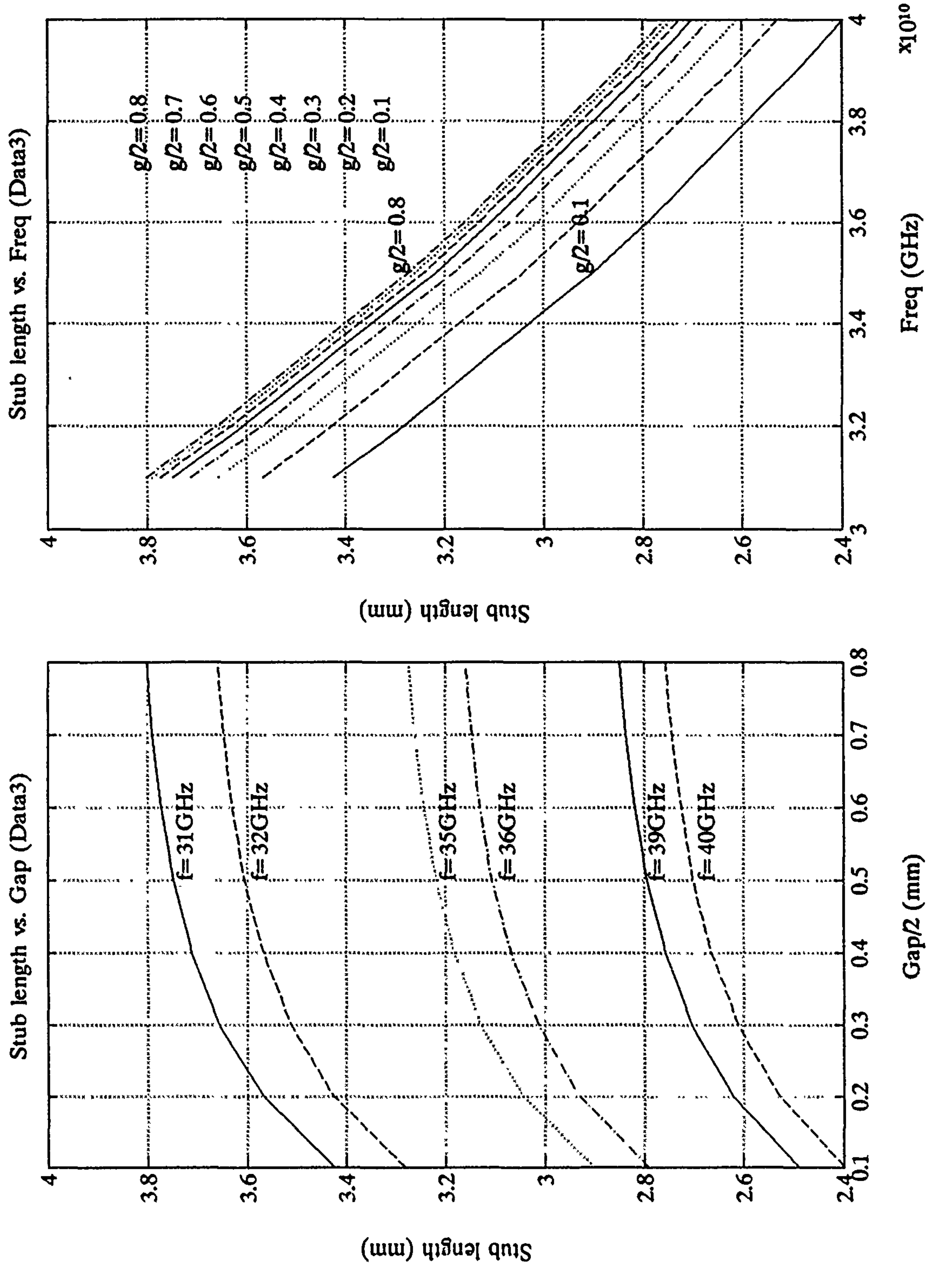

Figure 10. Stub lengths related to gap size and frequency

IV. DERIVATION OF THE PI–CIRCUIT REPRESENTATION OF THE DISCONTINUITY

A. EQUIVALENT NETWORK

The gap discontinuity is represented by a capacitive PI–network. This circuit is terminated on each side by an open–ended stub. The PI–circuit components are evaluated in terms of the admittance matrix, $[Y_{ij}]$, of the two–port discontinuity, as shown below.

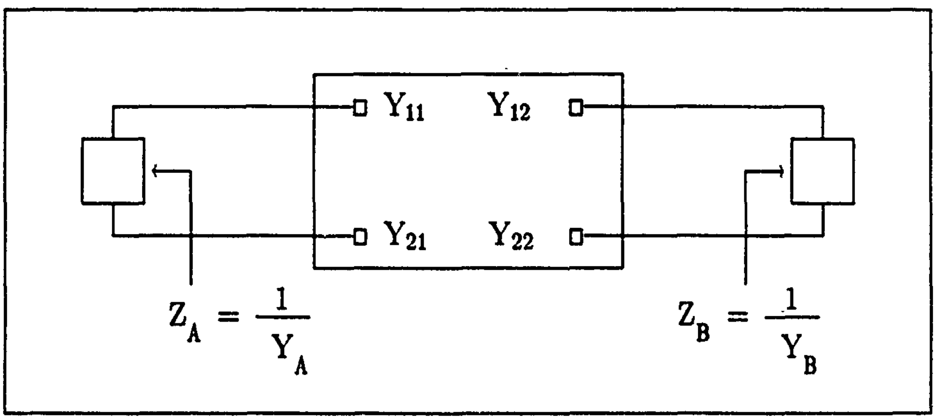

Figure 11. PI–Network

The admittance of an open line segment is:

$$Y_{in} = Y_{A,B} = jY_0 \tan\beta\ell, \quad (\ell = \text{strip line length})$$

From the 2–port admittance matrix,

$$I_1 = Y_{11}V_1 + Y_{12}V_2$$

$$I_2 = Y_{21}V_1 + Y_{22}V_2$$

$$\frac{I_1}{V_1} = Y_{11} + Y_{12}\frac{V_2}{V_1}$$

$$\frac{I_2}{V_2} = Y_{21}\frac{V_1}{V_2} + Y_{22}$$

$$\frac{V_1}{V_2} = \left[\frac{I_2}{V_2} - Y_{22}\right]\frac{1}{Y_{21}}$$

$$\frac{V_2}{V_1} = \frac{Y_{21}}{\left[\frac{I_2}{V_2} - Y_{22}\right]}$$

$$\frac{I_1}{V_1} = Y_{11} + Y_{12}\frac{Y_{21}}{\left[\frac{I_2}{V_2} - Y_{22}\right]}$$

But at resonance

$$\frac{V_1}{I_1} = -\frac{1}{Y_A}, \quad \frac{V_2}{I_2} = -\frac{1}{Y_B}$$

$$-Y_A - Y_{11} = \frac{Y_{12}Y_{21}}{-Y_B - Y_{22}}$$

$$\left[Y_{11} + Y_A\right]\left[Y_{22} + Y_B\right] - Y_{12}^2 = 0 \qquad (25)$$

This equation is used to calculate the equivalent circuit capacitances. The admittance–matrix values for the equivalent circuit parameters are as shown in Fig. 5.

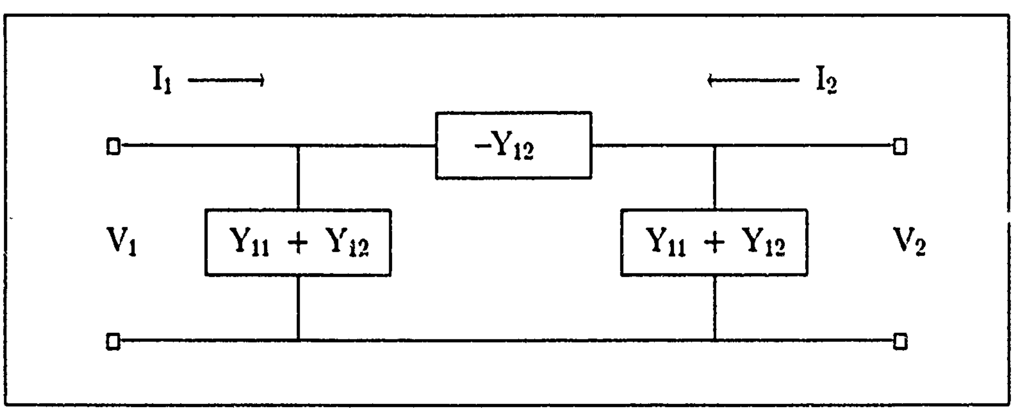

Figure 12. Admittance network

B. SUSPENDED STRIPLINE GAP CAPACITANCE

Figure 13 is the equivalent network of Fig. 1 which shows the configuration of the gap discontinuity in a suspended stripline. This network is enclosed in the central box in Fig. 14. In the computation procedure, stub lengths ℓ_1 are assumed and the corresponding frequency of resonance is found. Then a slightly different length ℓ_2 is employed to find the new resonance frequency. The resulting two solution values provide the necessary data for the calculation of the discontinuity capacitances, C_{gap} and C_{par}.

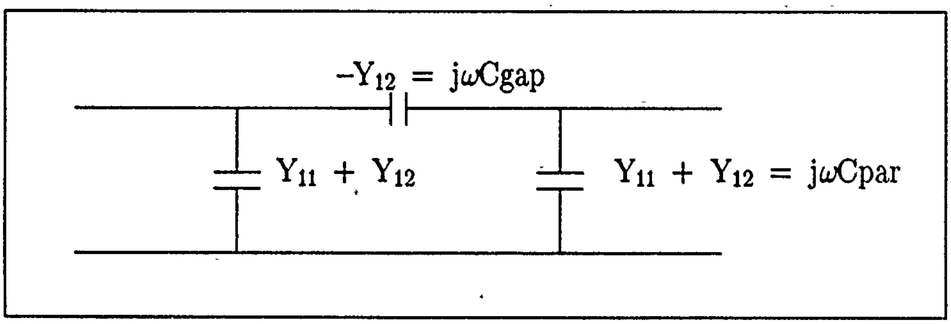

Figure 13. Network parameters

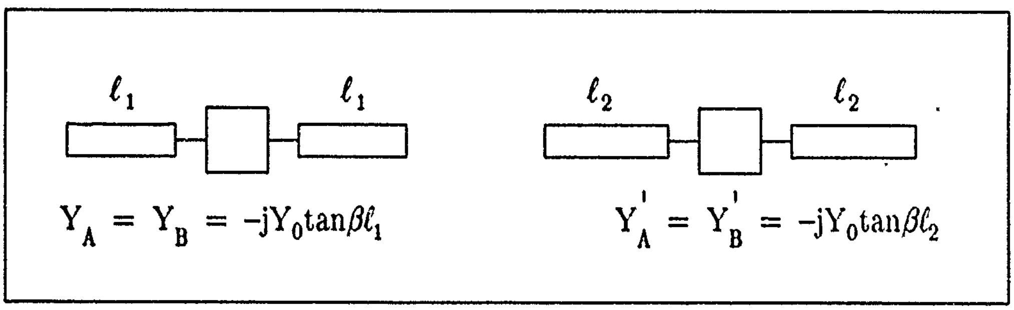

Figure 14. Analysis procedure

$$(Y_{11} + Y_A)(Y_{11} + Y_B) = Y_{12}^2 \tag{26a}$$

$$(Y_{11} + Y_A')(Y_{11} + Y_B') = Y_{12}^2 \tag{26b}$$

$$Y_{11}^2 + Y_{11}(Y_A + Y_B) + Y_AY_B = Y_{11}^2 + Y_{11}(Y_A' + Y_B') + Y_A'Y_B'$$

$$Y_{11} = \frac{Y_A' Y_B' - Y_A Y_B}{Y_A + Y_B - Y_A' - Y_B'} = -\frac{Y_A(f_1) + Y_A(f_2)}{2} \tag{27a}$$

$$Y_{12} = \sqrt{(Y_{11} + Y_A)(Y_{11} + Y_B)} = \pm \{Y_{11} + Y_A(f_1)\} \tag{27b}$$

TABLE 5. GAP CAPACITANCES WITH DATA 2 (SEC. III–B)*

g/2 \ f	86	94	102
0.05	0.1896	0.1893	0.2249
0.1	0.1417	0.1504	0.1667
0.15	0.1209	0.1257	0.1346
0.2	0.1154	0.1148	0.1236
0.25	0.1090	0.1073	0.1190
0.3	0.1017	0.1050	0.1101

TABLE 6. PARALLEL CAPACITANCES WITH DATA 2 (SEC. III–B)*

g/2 \ f	86	94	102
0.05	20.3573	21.5289	22.9300
0.1	16.8361	17.6024	18.5599
0.15	15.0875	15.7299	16.4805
0.2	14.1369	14.6720	15.3471
0.25	13.5670	14.0813	14.6777
0.3	13.2336	13.7098	14.2771

* In Tables 5 to 8, frequencies f are given in gigahertz, and the tabulated capacitances are in femtofarads.

TABLE 7. GAP CAPACITANCES WITH DATA 3 (SEC. III–B)*

g/2 \ f	32	36	40
0.1	1.4789	1.5487	0.9855
0.2	1.0326	1.1390	0.5812
0.3	0.8946	0.9906	0.4080
0.4	0.8200	0.8371	0.3403
0.5	0.7594	0.7638	0.2266
0.6	0.7176	0.7307	0.2156
0.7	0.6859	0.7012	0.1925
0.8	0.6594	0.6784	0.1688

TABLE 8. PARALLEL CAPACITANCES WITH DATA 3 (SEC. III–B)*

g/2 \ f	32	36	40
0.1	55.8182	60.9670	67.4308
0.2	45.8325	48.8567	53.0624
0.3	40.4891	42.7917	46.0020
0.4	37.3474	39.3528	41.8948
0.5	35.3625	37.1171	39.3973
0.6	34.0614	35.6390	37.7064
0.7	33.2005	34.6583	36.5680
0.8	32.6301	34.0021	35.8057

C. RESULTS

Tables 5 to 8 summarize the series and parallel equivalent–circuit capacitances of the gap discontinuity over the range of calculated dimensions and frequencies. This data is also shown in graphical form in Figs. 15 to 18. As may be seen in these Figures, both the series gap capacitance (C_{gap}) and the shunt parasitic capacitance (C_{par}) were found to decrese monotonically with gap length, at all frequencies. The plots of capacitance vs. frequency show, however, that while the parallel capacitance rises with frquency, for all system dimensions computed, the series gap capacitance C_{gap} rises to a maximum near the center of the K–band region, but C_{gap} shows a trend toward minimum values at mid–w–band frequencies.

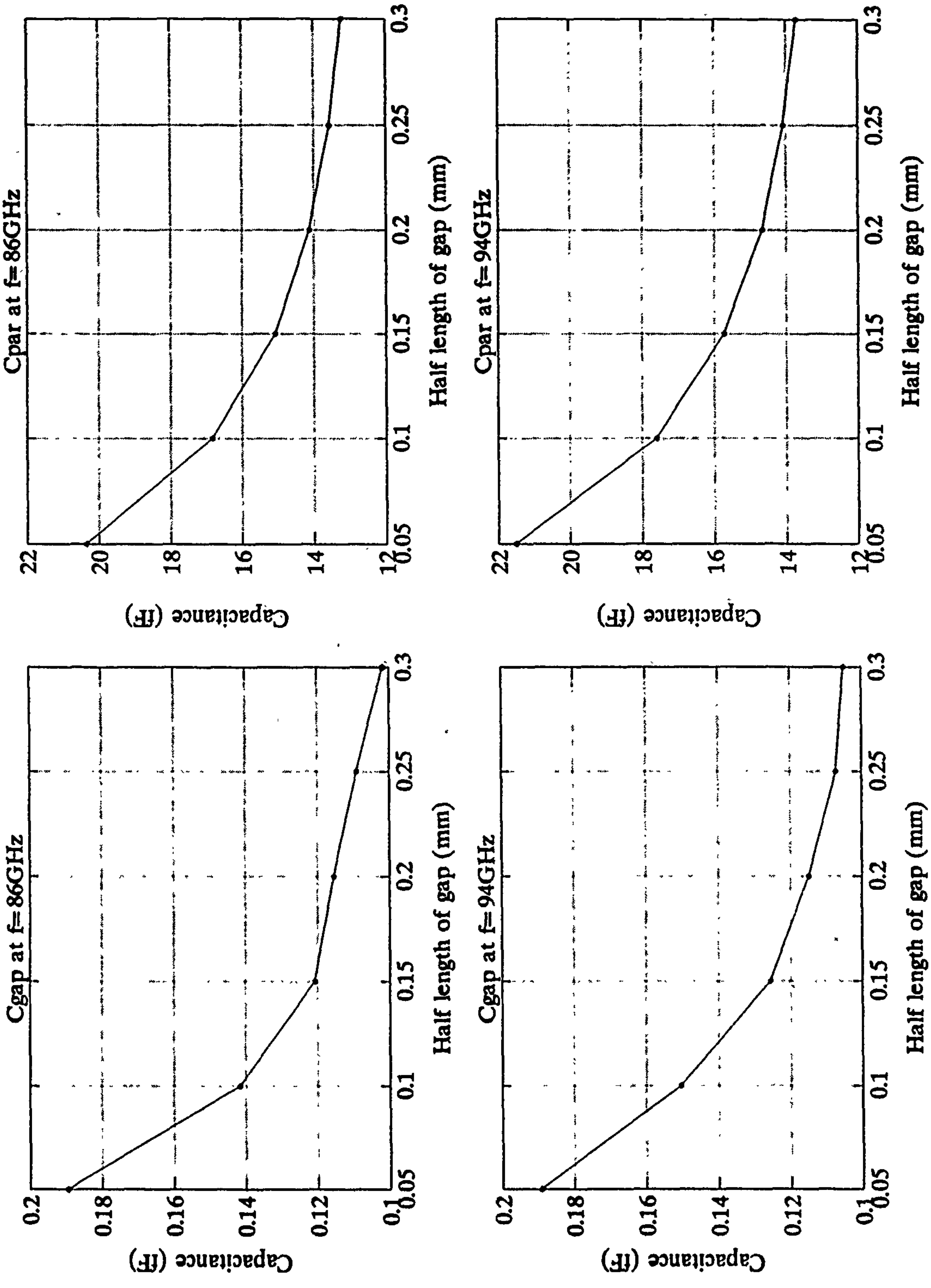

Figure 16. Capacitances at W-band

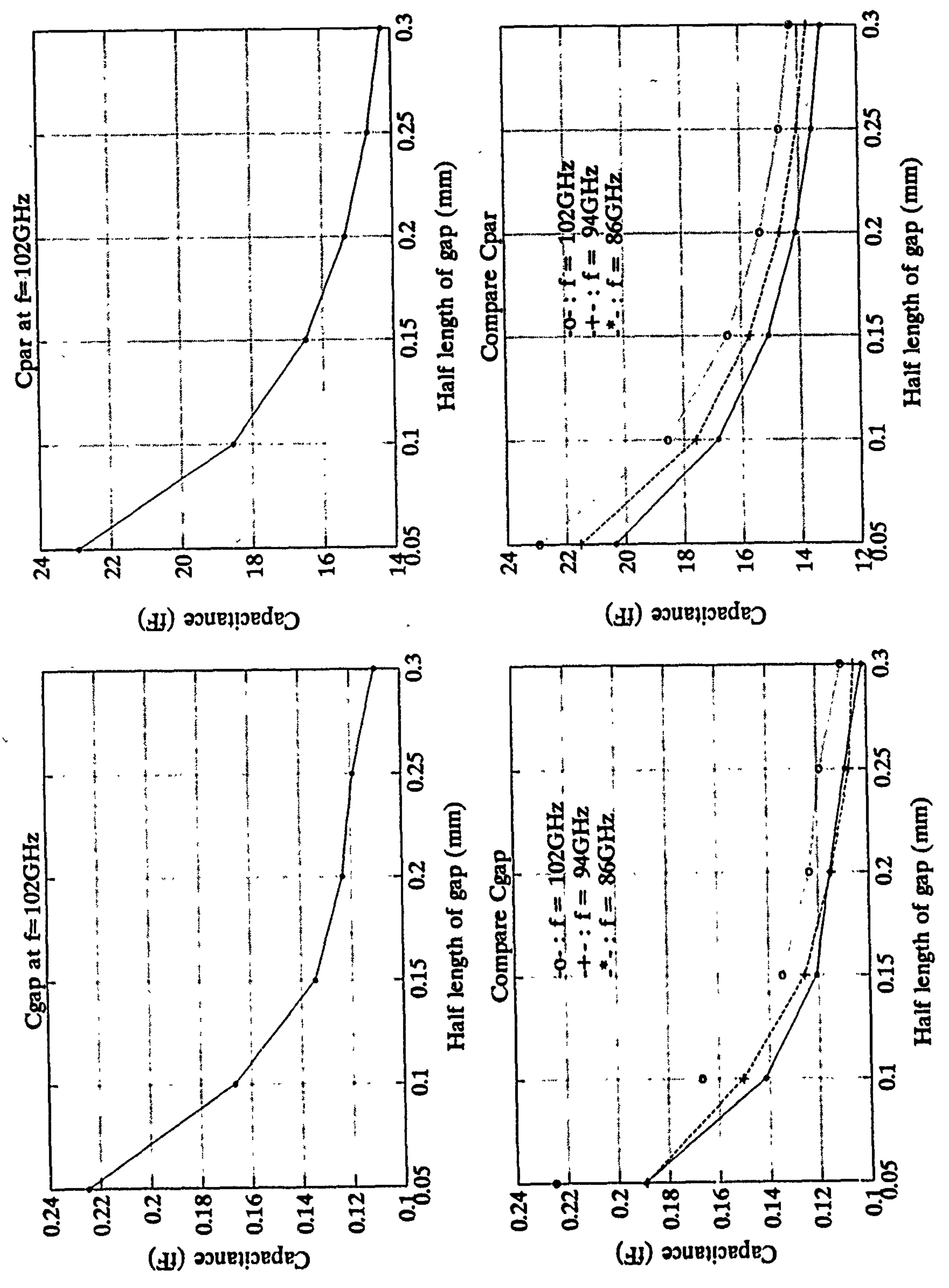

Figure 16. Continued

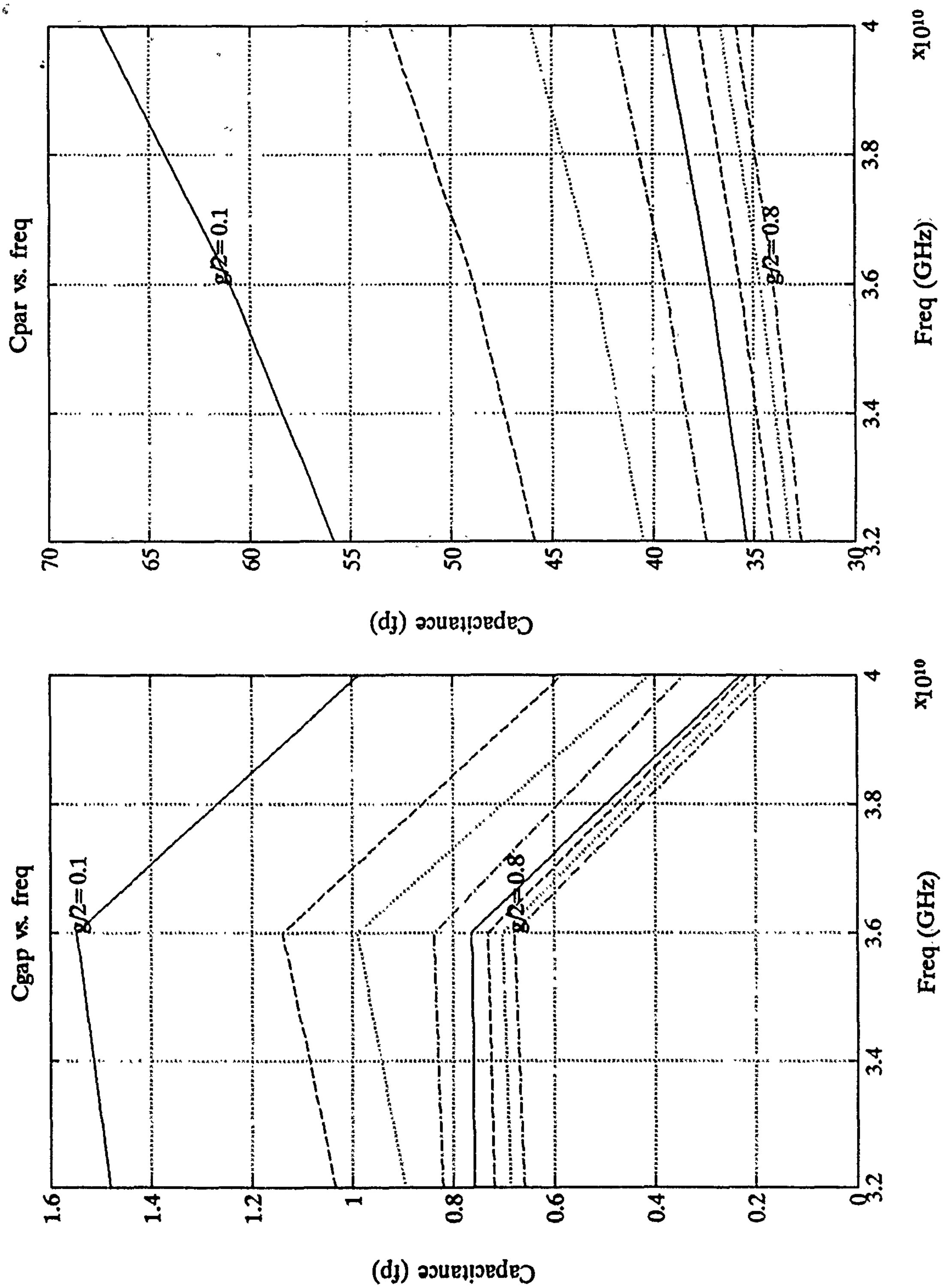

Figure 17. Capacitance vs. frequency at Ka–band

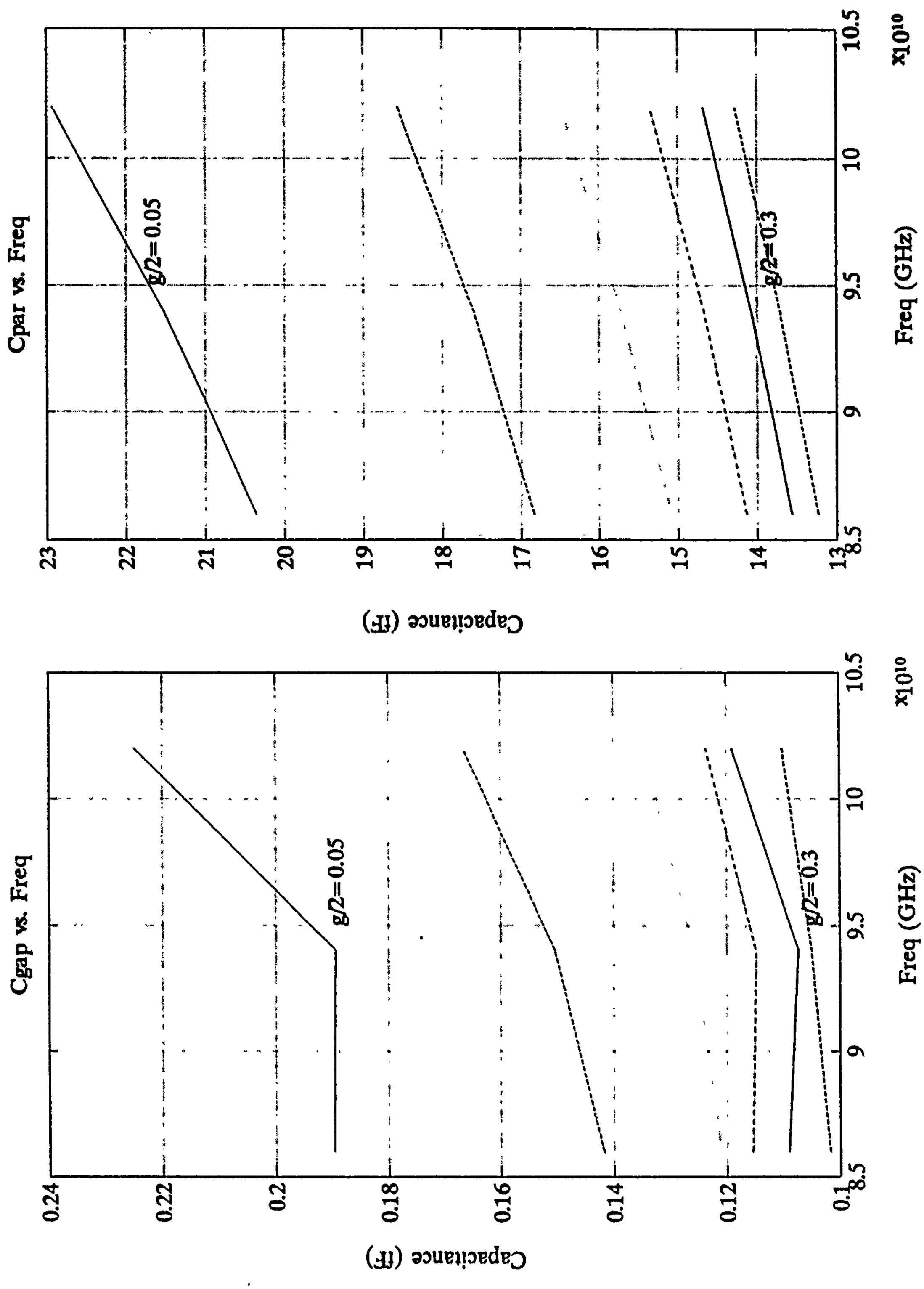

Figure 18. Capacitance vs. frequency at W-band

V. CONCLUSIONS

This thesis follows the methods originated by Itoh for the analysis of the suspended stripline resonator [Refs. 1 and 3], and for the equivalent circuit of the gap discontinuity [Ref. 4]. Some changes have been introduced in these approaches, however. A fully-shielded enclosure was employed, allowing the use of a finite Fourier transform in two coordinate directions. This change reduced the computation time significantly, while reproducing the results of the integral transform along the line axis.

The perturbed-resonator technique permitted the use of the strip current-density distributions suggested by Itoh [Ref. 1]. These are known to give accurate results in the Galerkin method. A calculation was made employing the resonator configuration used in [Ref. 5], which is the only known literature reference on the suspended stripline gap.

Table 5, Table 6, Fig. 16 and Fig. 18 shows the resulting parameters at W-band. Table 7, Table 8, Fig. 15 and Fig. 17 show the parameters at Ka-band. It is evident that all these capacitances are strongly frequency-dependent. Comparing these data with data from [Ref. 5], we see that the gap capacitances found in the present work range from 0.1 – 1.5 femtofarads. These gap capacitances are smaller by an order of magnitude than those found by Rong and Li [Ref. 5], but the accuracy of the latter work has not been confirmed. When the gap is widened, the capacitance changes at a rate comparable with that in [Ref. 5]. The parallel capacitances found here range from 13 – 70 femtofarads. This parallel capacitance shows an inverse

dependence on gap length, unlike that of [Ref. 5]. The reason for this discrepancy is not known, although it is felt that the capacitance variation found in the present work is correct.

The two–frequency calculation for each capacitance used here introduces some error, but this should be small for small computed frequency differences. In any event, the circuit–equivalent capacitances found in this way should be accurate at a frequency intermediate between the two frequencies of the pair employed in each case.

Recommendation: In attempting to use Itoh's method of perturbed resonators having the same frequency, the determinant of Eqs. (17) did not go to zero. The reason for this failure should be determined, so that an ideally accurate computation of equivalent–circuit parameters at a well–defined single frequency can be made.

APPENDIX B

FOURIER TRANSFORMS OF THE ASSUMED CURRENT DISTRIBUTIONS

The evaluation of the Fourier–transformed forms of the strip current densities is shown in detail below:

A. CONTINUOUS STRIP

The coördinate form of the current distributions in Fig. 2.

$$J_1(x) = \frac{1}{2w}\left[1 + \left|\frac{x}{w}\right|^3\right], \qquad -w \le x \le w \tag{B–1a}$$

$$J_2(z) = \frac{1}{\ell}\cos\frac{\pi z}{2\ell}, \qquad -\ell \le z \le \ell \tag{B–1b}$$

$$J_3(x) = \frac{1}{w}\sin\frac{\pi x}{w}, \qquad -w \le x \le w \tag{B–1c}$$

$$J_4(z) = \frac{z}{2\ell^2}, \qquad -\ell \le z \le \ell \tag{B–1d}$$

The Fourier transform is defined to be:

$$\tilde{\phi}(\alpha) = \int_{-\infty}^{\infty} \phi(x) e^{j\alpha x} dx \tag{B–2}$$

The Fourier transforms are calculated as shown:

$$\tilde{J}_1(n) = \int_{-\infty}^{\infty} J_1(x) e^{jk_n x} dx, \tag{B–3a}$$

$$\tilde{J}_2(\beta) = \int_{-\infty}^{\infty} J_2(z) e^{j\beta z} dz, \tag{B–3b}$$

$$\tilde{J}_3(n) = \int_{-\infty}^{\infty} J_3(x) e^{jk_n x} dx, \tag{B–3c}$$

$$\tilde{J}_4(\beta) = \int_{-\infty}^{\infty} J_4(z) e^{j\beta z} dz, \tag{B–3d}$$

The Fourier transforms of the basic current distributions are:

$$\tilde{J}_1(n) = \int_{-\infty}^{\infty} \frac{1}{2w}\left[1 + \left|\frac{x}{w}\right|^3\right] e^{jk_n x} dx, \qquad -w \le x \le w, \tag{B-4a}$$

$$\tilde{J}_2(\beta) = \int_{-\infty}^{\infty} \frac{1}{\ell} \cos\frac{\pi z}{2\ell} e^{j\beta z} dz, \qquad -\ell \le z \le \ell, \tag{B-4b}$$

$$\tilde{J}_3(n) = \int_{-\infty}^{\infty} \frac{1}{w} \cdot \sin\frac{\pi x}{w} e^{jk_n x} dx, \qquad -w \le x \le w, \tag{B-4c}$$

$$\tilde{J}_4(\beta) = \int_{-\infty}^{\infty} \frac{z}{2\ell^2} e^{j\beta z} dz, \qquad -\ell \le z \le \ell, \tag{B-4d}$$

The Fourier transforms are calculated as shown below:

From Eq. (B-4a)

$$\tilde{J}_1(n) = \int_{-\infty}^{\infty} \frac{1}{2w}\left[1 + \left|\frac{x}{w}\right|^3\right] e^{jk_n x} dx = \frac{1}{2w} \cdot \int_{-w}^{w} \left[1 + \left|\frac{x}{w}\right|^3\right] e^{jk_n x} dx$$

$$= \frac{1}{2w} \cdot \left[\int_{-w}^{w} e^{jk_n x} dx + \frac{1}{w^3}\int_{-w}^{w} |x|^3 e^{jk_n x} dx\right] \tag{B-5a}$$

The first term of Eq. (B-5a) is evaluated as follow:

$$\int_{-w}^{w} e^{jk_n x} dx = \frac{1}{jk_n} e^{jk_n x}\Big|_{x=-w}^{w}$$

$$= \frac{1}{jk_n}(e^{jk_n w} - e^{-jk_n w})$$

$$= \frac{1}{jk_n}(\cos k_n w + j\sin k_n w - \cos k_n w + j\sin k_n w)$$

$$= \frac{2}{k_n}\sin k_n w. \tag{B-5b}$$

The second term of Eq. (B-5a) is evaluated as follow:

$$\int_{-w}^{w} |x|^3 e^{jk_n x} dx \tag{B-5c}$$

Use $\int u dv = uv - \int v du$

For positive in Eq. (B–5c) we have:

$$\int_0^w x^3 e^{jk_n x} dx$$

$$= x^3 \frac{e^{jk_n x}}{jk_n} - \int_0^w 3x^2 \frac{e^{jk_n x}}{jk_n} dx$$

$$= \frac{x^3 e^{jk_n x}}{jk_n} - \frac{3}{jk_n}\left\{\frac{x^2 e^{jk_n x}}{jk_n} - \int_0^w 2x \frac{e^{jk_n x}}{jk_n} dx\right\}$$

$$= \frac{x^3 e^{jk_n x}}{jk_n} - \frac{3}{jk_n}\left\{\frac{x^2 e^{jk_n x}}{jk_n} - \frac{2}{jk_n}\left[\frac{x e^{jk_n x}}{jk_n} - \int_0^w \frac{e^{jk_n x}}{jk_n} dx\right]\right.$$

$$= \frac{x^3 e^{jk_n x}}{jk_n} + \frac{3x^2 e^{jk_n x}}{k_n^2} - \frac{6}{k_n^2}\left[\frac{x e^{jk_n x}}{jk_n} + \frac{e^{jk_n x}}{k_n^2}\right]\Bigg|_{x=0}^{w}$$

$$= \frac{w^3 e^{jk_n w}}{jk_n} + \frac{3w^2 e^{jk_n w}}{k_n^2} - \frac{6}{k_n^2}\left[\frac{w e^{jk_n w}}{jk_n} + \frac{e^{jk_n w}}{k_n^2}\right] + \frac{6}{k_n^4}$$

$$= -j\frac{w^3 e^{jk_n w}}{k_n} + \frac{3w^2 e^{jk_n w}}{k_n^2} + j\frac{6w e^{jk_n w}}{k_n^3} - \frac{6e^{jk_n w}}{k_n^4} + \frac{6}{k_n^4} \quad \text{(B–5d)}$$

For negative x in Eq. (B–5c) we have:

$$-\int_{-w}^{0} x^3 e^{jk_n x} dx$$

$$= -\left[\frac{x^3 e^{jk_n x}}{jk_n} + \frac{3x^2 e^{jk_n x}}{k_n^2} - \frac{6}{k_n^2}\left[\frac{x e^{jk_n x}}{jk_n} + \frac{e^{jk_n x}}{k_n^2}\right]\right]\Bigg|_{x=-w}^{0}$$

$$= \frac{6}{k_n^4} + \left\{\frac{-w^3 e^{-jk_n w}}{jk_n} + \frac{3w^2 e^{-jk_n w}}{k_n^2} - \frac{6}{k_n^2}\left[\frac{-w e^{-jk_n w}}{jk_n} + \frac{e^{-jk_n w}}{k_n^2}\right]\right\}$$

$$= \frac{6}{k_n^4} + j\frac{w^3 e^{-jk_n w}}{k_n} + \frac{3w^2 e^{-jk_n w}}{k_n^2} - j\frac{6w e^{-jk_n w}}{k_n^3} - \frac{6e^{-jk_n w}}{k_n^4} \quad \text{(B–5e)}$$

Now we add up together Eq. (B–5b) Eq. (B–5d) and Eq. (B–5e) into Eq. (B–5a)

$$\tilde{J}_1(n) = \frac{1}{2w}\Big[\frac{2\sin k_n w}{k_n} + \frac{1}{w^3}\cdot\Big\{ -j\frac{w^3 e^{jk_n w}}{k_n} + \frac{3w^2 e^{jk_n w}}{k_n^{\ 2}}$$

$$+ j\frac{6we^{jk_n w}}{k_n^{\ 3}} - \frac{6e^{jk_n w}}{k_n^{\ 4}} + \frac{6}{k_n^{\ 4}} + \frac{6}{k_n^{\ 4}} + j\frac{w^3 e^{-jk_n w}}{k_n} + \frac{3w^2 e^{-jk_n w}}{k_n^{\ 2}}$$

$$- j\frac{6we^{-jk_n w}}{k_n^{\ 3}} - \frac{6e^{-jk_n w}}{k_n^{\ 4}}\Big\}\Big]$$

$$= \frac{1}{2w}\Big[\frac{2\sin k_n w}{k_n} + \frac{1}{w^3}\cdot\Big\{ -j\frac{w^3 e^{jk_n w}}{k_n} + j\frac{w^3 e^{-jk_n w}}{k_n} + \frac{3w^2 e^{jk_n w}}{k_n^{\ 2}}$$

$$+ \frac{3w^2 e^{-jk_n w}}{k_n^{\ 2}} + j\frac{6we^{jk_n w}}{k_n^{\ 3}} - j\frac{6we^{-jk_n w}}{k_n^{\ 3}} - \frac{6e^{jk_n w}}{k_n^{\ 4}} - \frac{6e^{-jk_n w}}{k_n^{\ 4}} + \frac{12}{k_n^{\ 4}}\Big\}\Big] \qquad \text{(B–5f)}$$

Now we consider Euler's equation

$$e^{jk_n w} - e^{-jk_n w} = 2j\sin k_n w$$

$$e^{jk_n w} + e^{-jk_n w} = 2\cos k_n w$$

$$\tilde{J}_1(n) = \frac{1}{2w}\Big[\frac{2\sin k_n w}{k_n} + \frac{1}{w^3}\cdot\Big\{-j\frac{w^3(2j\sin k_n w)}{k_n} + \frac{3w^2(2\cos k_n w)}{k_n^{\ 2}}$$

$$+ j\frac{6w(2j\sin k_n w)}{k_n^{\ 3}} - \frac{6(2\cos k_n w)}{k_n^{\ 4}} + \frac{12}{k_n^{\ 4}}\Big\}\Big]$$

$$= \frac{\sin k_n w}{k_n w} + \frac{1}{2w^4}\cdot\Big\{\frac{2w^3\sin k_n w}{k_n} + \frac{6w^2\cos k_n w}{k_n^{\ 2}} - \frac{12w\sin k_n w}{k_n^{\ 3}}$$

$$- \frac{12\cos k_n w}{k_n^{\ 4}} + \frac{12}{k_n^{\ 4}}\Big\}$$

$$= \frac{2\sin k_n w}{k_n w} + \frac{3\cos k_n w}{k_n^{\ 2} w^2} - \frac{6\sin k_n w}{k_n^{\ 3} w^3} - \frac{6\cos k_n w}{k_n^{\ 4} w^4} + \frac{6}{k_n^{\ 4} w^4}$$

$$= \frac{2\sin k_n w}{k_n w} + \frac{3}{k_n^{\ 2} w^2}\Big\{\cos k_n w - \frac{2\sin k_n w}{k_n w} + \frac{2(1 - \cos k_n w)}{k_n^{\ 2} w^2}\Big\} \qquad \text{(B–5g)}$$

$$= \frac{1}{2\ell^2}\left[\frac{ze^{j\beta z}}{j\beta} - \int_{-\ell}^{\ell}\frac{e^{j\beta z}}{j\beta}dz\right]$$

$$= \frac{1}{2\ell^2}\left[\frac{ze^{j\beta z}}{j\beta} - \frac{e^{j\beta z}}{(j\beta)^2}\right]\Bigg|_{z=-\ell}^{\ell}$$

$$= \frac{1}{2\ell^2}\left\{\frac{\ell e^{j\beta\ell}}{j\beta} - \frac{e^{j\beta\ell}}{(j\beta)^2} - \left[\frac{-\ell e^{-j\beta\ell}}{j\beta} - \frac{e^{-j\beta\ell}}{(j\beta)^2}\right]\right\}$$

$$= \frac{1}{2\ell^2}\left\{\frac{\ell}{j\beta}(e^{j\beta\ell} + e^{-j\beta\ell}) + \frac{1}{\beta^2}(e^{j\beta\ell} - e^{-j\beta\ell})\right\}$$

$$= \frac{1}{2\ell^2}\left\{\frac{\ell}{j\beta}2\cos\beta\ell + \frac{1}{\beta^2}2j\sin\beta\ell\right\}$$

$$= -j\left[\frac{\cos\beta\ell}{\beta\ell} - \frac{\sin\beta\ell}{(\beta\ell)^2}\right] \qquad \text{(B-8)}$$

Finally the current distributions are found to be:

From Eq. (B-5f) and Eq. (B-6)

$$\tilde{J}_z(k_n,\beta) = \tilde{J}_1(n)\cdot\tilde{J}_2(\beta)$$

$$= \left[\frac{2\sin k_n w}{k_n w} + \frac{3}{k_n{}^2 w^2}\left\{\cos k_n w - \frac{2\sin k_n w}{k_n w} + \frac{2(1-\cos k_n w)}{k_n{}^2 w^2}\right\}\right]\frac{4\pi\cos\beta\ell}{\pi^2-4(\beta\ell)^2} \qquad \text{(B-9)}$$

From Eq. (B-7) and Eq. (B-8)

$$\tilde{J}_x(k_n,\beta) = \tilde{J}_3(n)\cdot\tilde{J}_4(\beta)$$

$$= j\frac{2\pi\sin k_n w}{\pi^2 - (k_n w)^2}\left\{-j\left[\frac{\cos\beta\ell}{\beta\ell} - \frac{\sin\beta\ell}{(\beta\ell)^2}\right]\right\}$$

$$= \frac{2\pi\sin k_n w}{\pi^2 - (k_n w)^2}\left[\frac{\cos\beta\ell}{\beta\ell} - \frac{\sin\beta\ell}{(\beta\ell)^2}\right] \qquad \text{(B-10)}$$

B. RESONATOR WITH GAP

Asume $J_x = 0$

$$J_z = c_1 J_{z1} + c_2 J_{z2}$$

$$J_{z1} = J_{z1}(z) \cdot J_{zx}(x)$$

$$J_{z2} = J_{z2}(z) \cdot J_{zx}(x)$$

In both open-ended line segments of same length, current $J_{z1}(z)$ is chosen to have the form shown in Fig. 19.

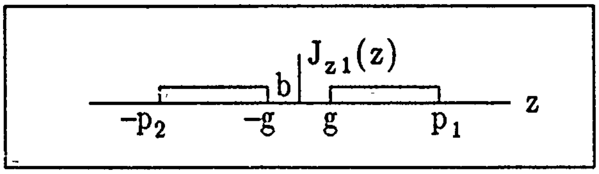

Figure 19. Current distribution of J_{z1}

$$J_{z1}(z) = b, \qquad |x| \le a, \ |z| \le \ell$$

Normalization of $J_{z1}(z)$ leads to:

$$(p_1 - g) + (p_2 - g)b = 1$$

$$b = \frac{1}{p_1 + p_2 - 2g}$$

$$J_{z1}(z) = b = \frac{1}{p_1 + p_2 - 2g} \quad . \tag{B-11a}$$

Using $J_{z2}(z)$ from Fig. 3, we have:

Let $d_1 = p_1 - g, \qquad d_2 = p_2 - g$

$$J_{z2}(z) = \begin{cases} -\frac{1}{2d_2} \cdot \sin(\frac{\pi z}{d_2} + \frac{g\pi}{d_2}), & -p_2 < z < -g \\ \frac{1}{2d_2} \cdot \sin(\frac{\pi z}{d_2} + \frac{g\pi}{d_2}), & g < z < p_1 \end{cases} \tag{B-11b}$$

The Fourier transform from Eq. (B-11a) is:

$$J_{z1}(\beta) = \int_{-\infty}^{\infty} J_{z1}(z) e^{j\beta z} dz$$

APPENDIX C.

PROGRAM LISTINGS

A. RESONATOR FREQUENCY

```
      program SSMSL
c     This program calculates resonator frequency
c
      integer i, n, m, compare, count
      real*8 a, w, l, d, t, h, Er, f
      real*8 kn, beta, omega, rl
      real*8 pi, E0, Mu0, c
      real*8 gam1s, gam2s
      real*8 Jzin, Jzkn, Jzbe, Jz1, Jxkn, Jxbe, Jx1
      real*8 cmp, limit, odlf, newf, limf
c
      logical llog
c
      complex*16 gama1, gama2, gama3, Ct1, Ct2, Ct3
      complex*16 Zen, Zenr, Zed, Zer, Zhn, Zhd, Zhnr, Zhr, Zden
      complex*16 Ze, Zh, Zzz, Zzx, Zxz, Zxx
      complex*16 K11, K12, K22, j, sk11, sk12, sk22, det
      character*8 fname
      character*14 sname
c
      open(1,file='data.in')
      print*, 'Enter output data file name  fn'
      read*, fname
      open(2, file=fname)
      sname = fname // '.plt'
      open(3, file=sname)
      write(2,*) '     file name = ',fname
      write(3,*) '     file name = ',sname
c
c     parameter
      c = 3.e8
      j = cmplx(0.,1.)
      pi = 4.*atan(1.)
      E0 = 1.e-9/(36.*pi)
      Mu0 = 4.*pi*1.e-7
      limit = 1.e-2
      compare = 1
      count = 1
      llog = .true.
```

```
      call READF(w,l,a,d,t,h,Er)
c
      write(2,22) w,l,a,d,t,h,Er
22    format(t5,'Unit : milimiter'
     &     ,/,t5,'Micro strip line width and length : ',2(e12.6,3x)
     &     ,/,t5,'Rasonator width                    : ',e12.6
     &     ,/,t5,'heights of layers 1, 2 and 3       : ',3(e12.6,3x)
     &     ,/,t5,'Permittivity of substrate Er       : ',f7.3)
c
c     Decide propagation constant Beta
c     Applying a root - seeking process
c
c     Calculate the summation
c
      print*, 'Enter the number of outer summation loop'
      read*, n
c     n = 20
      write(2,*) 'The number of outer summation loop = ',n
      write(3,*) 'The number of outer summation loop = ',n
c
      print*, 'Enter the number of inner summation loop'
      read*, m
      write(2,*) 'The number of inner summation loop = ',m
      write(3,*) 'The number of inner summation loop = ',m
      rl = 10.*l
c
c     initial value
1     print*, 'Enter initial frequency GHz'
      read*, f
      f = f*1.e9
c
11    print*, 'Frequency = ',f
      write(2,*) 'Frequency = ',f
c
      omega = 2.*pi*f
c
      K11 = cmplx(0.,0.)
      K12 = cmplx(0.,0.)
      K22 = cmplx(0.,0.)
c
      do 20 i = 1, n
        kn = (i - .5)*pi/a
c
        Jzin = cos(kn*w) - 2.*sin(kn*w)/(kn*w)
     &          + 2.*(1-cos(kn*w))/(kn*w)**2
        Jzkn = 2.*sin(kn*w)/(kn*w) + 3.*Jzin/(kn*w)**2
c
        Jxkn = 2*pi*sin(kn*w)/(pi**2 - (kn*w)**2)
c
c       Compute summation loop for beta
```

```
      sk11 = cmplx(0.,0.)
      sk12 = cmplx(0.,0.)
      sk22 = cmplx(0.,0.)
c
        do 40 im = 1,m
          beta = (real(im) - .5)*pi/rl
c
c         Calculate the gamma1 and gamma3
c
          gam1s = kn**2 + beta**2 - E0*Mu0*omega**2
c
          call gamct(gama1,gam1s,Ct1,d)
c
          call gamct(gama3,gam1s,Ct3,h)
c
          gam2s = kn**2 + beta**2 - E0*Mu0*Er*omega**2
c
          call gamct(gama2,gam2s,Ct2,t)
c
c         Calculate Ze
c
          Zen = gama2*Ct1/Er + gama1*Ct2
          Zenr = -j/(omega*E0)
c
          Zed = Ct1*Ct2 + Ct1*Ct3*gama2/gama3/Er
     &          + Ct2*Ct3 + Er*gama1/gama2
          Ze = Zenr*Zen/Zed
c
c         Calculate Zh
c
          Zhn = gama1*Ct1 + gama2*Ct2
c
          Zhd = gama1*Ct1*gama2*Ct2 + gama1*Ct1*gama3*Ct3
     &          + gama2*Ct2*gama3*Ct3 + gama2**2
          Zhnr = j*omega*Mu0
          Zh = Zhnr*Zhn/Zhd
c
c         Calculate
c
       Zden = kn**2 + beta**2
       Zzz = -(Ze*beta**2 + Zh*kn**2)/Zden
       Zzx = -kn*beta*(Ze - Zh)/Zden
       Zxz = Zzx
       Zxx = -(Ze*kn**2 + Zh*beta**2)/Zden
c
c      Calculate Jz1
c
       Jzbe = 4.*pi*cos(beta*l)/(pi**2 - (2.*beta*l)**2)
c
       Jz1 = Jzkn*Jzbe
```

```
c         Calculate Jxl
c
          Jxbe = cos(beta*l)/(beta*l) - sin(beta*l)/(beta*l)**2
          Jxl = Jxkn*Jxbe
c
c            Calculate Matrix coefficient
c
        sk11 = sk11 + Jzl*Zzz*Jzl
        sk12 = sk12 + Jzl*Zzx*Jxl
        sk22 = sk22 + Jxl*Zxx*Jxl
c
40      continue
c
        K11 = K11 + sk11
        K12 = K12 + sk12
        K22 = K22 + sk22
c
20      continue
c
        print*, 'check K11 = ',K11
        write(2,*) 'check K11 = ',K11
        print*, 'check K12 = ',K12
        write(2,*) 'check K12 = ',K12
        print*, 'check K22 = ',K22
        write(2,*) 'check K22 = ',K22
c
        det = K11*K22 - K12*K12
        print*, 'determinent = ',det
        write(2,*) 'determinent = ',det
c
        call fdsort(f,det,count)
        count = count + 1

        if(llog) then
c         print*, 'Make sure opposite sign between new and old one'
c         print*, 'Not opposite sign then Enter  9 '
c         print*, 'Opposite sign      then Enter  0'
c         read*, ijk
          if(ijk.eq.9) then
            oldf = f
            go to 1
          endif
          llog = .false.
        endif
c
        cmp = real(det)
        limf = abs(f - oldf)
c
        print*, 'check limit freq ',limf
        write(2,*) ' check limit freq = ',limf
```

```
c      ****************************************************
c
       subroutine slval(fun,oxv,xv,newxv,sn)
c
       integer sn
       real*8 fun,oxv,xv,newxv,posxv,negxv
c
       if(sn .eq. 1) then
         if(fun .gt. 0) then
           posxv = xv
           negxv = oxv
         else
           negxv = xv
           posxv = oxv
         endif
         newxv = (posxv + negxv)/2.
         sn = sn + 2
       else
         if(fun .gt. 0) then
           posxv = xv
         else
           negxv = xv
         endif
         newxv = (posxv + negxv)/2.
       endif
c
       return
       end
c
c
c
c      ********************************************************
c
       subroutine fdsort(fqy,sdet,icount)
c
       integer icount, ic
c
       real*8 freqy(100),fqy,rtemp, magdet, tfqy
c
       complex*16 detmt(100),sdet,ctemp, tsdet

       tfqy = fqy
       tsdet = sdet
c
       if(icount .eq. 1) then
         freqy(1) = tfqy
         detmt(1) = tsdet
         elseif(icount .ne. 100) then
```

```
          do 10 i = 1, icount-1
            rtemp = freqy(i)
            ctemp = detmt(i)
c
            if(rtemp .gt. tfqy) then
              freqy(i) = tfqy
              tfqy = rtemp
              detmt(i) = tsdet
              tsdet = ctemp
            endif
c
10        continue
c
          freqy(icount) = tfqy
          detmt(icount) = tsdet
          ic = icount
c
        elseif(icount .eq. 100) then
          write(3,110)
110       format(//,t5,'Frequency',t20,'Mag of det',t35,'Determinent')
c
          do 20 j = 1,ic
            magdet = sqrt(real(detmt(j))**2 + aimag(detmt(j))**2)
            write(3,210) freqy(j),magdet,detmt(j)
210         format(t5,f15.2,t20,f15.3,t35,2(e15.8))
20        continue
        endif
c
        return
        end
```

```
c           Calculate Zh
c
            Zhn = gama1*Ct1 + gama2*Ct2
c
            Zhd = gama1*Ct1*gama2*Ct2 + gama1*Ct1*gama3*Ct3
     &           + gama2*Ct2*gama3*Ct3 + gama2**2
            Zhnr = j*omega*Mu0
            Zh = Zhnr*Zhn/Zhd
c
            trmn = -(B(m)**2*Ze + kn**2*Zh)*Jzkn**2/(B(m)**2 + kn**2)
            sum = trmn + sum
c
20        continue
c
          mag(m) = sqrt(real(sum)**2 + aimag(sum)**2)
c
          print71, m,B(m),mag(m),sum
          write(2,71) m,B(m),mag(m),sum
71        format(2x,i2,1x,f12.6,1x,f12.6,1x,2(f12.6,1x))
10      continue
c
        do 30 m = 2, (max-1)
          if(mag(m).lt.mag(m-1) .and. mag(m).lt.mag(m+1)) then
            print*, 'Suspended stripline BETA = ',B(m)
            write(2,*)
            write(2,*) 'Suspended stripline BETA = ',B(m)
            be = B(m)
          endif
30      continue
c
        Ereff = (be*c/omega)**2
        print*, 'Ereff = ',Ereff
        write(2,*) 'Ereff = ',Ereff
c
        dth = d + t + h
        call impd(Z0,Ereff,a,dth,t,w)
c
        print*, 'Z0 = ',Z0
        write(2,*) 'Z0 = ',Z0
        close(1)
        close(2)
c
        write(3,95) f, be, Ereff, Z0
95      format(2x,e12.6,2x,f8.3,2x,f9.6,2x,f9.5)
c
        go to 11
c
999     close(3)
c
        stop
        end
```

Input data file for frequency

```
'bezdata.out'
'f31' 31
'f32' 32
'f35' 35
'f36' 36
'f39' 39
'f40' 40
'f41' 41
'f85' 85
'f86' 86
'f93' 93
'f94' 94
'f101' 101
'f102' 102
```

Input data file for strip line demensions

```
Data 2.
microstip line width and length        :0.60000   0.00000
Waveguide width                            :1.27000
the height of layers 1, 2 and 3        :0.31800   0.12700   0.19000
the permittivity of substrate         :002.220

Data 3.
microstip line width and length        :1.50000   0.00000
Waveguide width                            :3.56000
the height of layers 1, 2 and 3        :0.76300   0.12700   0.89000
the permittivity of substrate         :002.220
```

Output data file

Frequency	Beta	Ereff	Z0
.310000E+11	683.772	1.109129	91.81764
.320000E+11	705.829	1.109129	91.81764
.350000E+11	772.001	1.109129	91.81764
.360000E+11	794.058	1.109129	91.81764
.390000E+11	860.229	1.109129	91.81764
.400000E+11	887.601	1.122532	91.26783
.410000E+11	909.792	1.122532	91.26783
.850000E+11	1953.919	1.204642	82.52280
.860000E+11	1976.906	1.204642	82.52280
.930000E+11	2137.817	1.204642	82.52280
.940000E+11	2160.805	1.204642	82.52280
.101000E+12	2321.716	1.204642	82.52280
.102000E+12	2344.703	1.204642	82.52280

Data file for input (frequency, beta, Ereff, Z0)

'f32'	32	31	705.829	683.772	1.109129	91.81764	8
'f36'	36	35	794.058	772.001	1.109129	91.81764	8
'f40'	40	39	887.601	860.229	1.109129	91.81764	8
'f86'	86	85	1976.906	1953.919	1.204642	82.5228	6
'f94'	94	93	2160.805	2137.817	1.204642	82.5228	6
'f02'	102	101	2344.703	2321.716	1.204642	82.5228	6

Data file for input (resonance stub length)

0.1	'gp1'	3.280426	3.423938
0.2	'gp2'	3.425125	3.567502
0.3	'gp3'	3.511975	3.655768
0.4	'gp4'	3.567063	3.711716
0.5	'gp5'	3.604022	3.748665
0.6	'gp6'	3.629065	3.773567
0.7	'gp7'	3.646109	3.790344
0.8	'gp8'	3.657755	3.801590
0.1	'gp1'	2.789856	2.900597
0.2	'gp2'	2.929428	3.042618
0.3	'gp3'	3.013024	3.128288
0.4	'gp4'	3.067654	3.181847
0.5	'gp5'	3.104645	3.218735
0.6	'gp6'	3.129601	3.244049
0.7	'gp7'	3.146843	3.261261
0.8	'gp8'	3.158684	3.272965
0.1	'gp1'	2.398560	2.490021
0.2	'gp2'	2.529320	2.622116
0.3	'gp3'	2.611054	2.704331
0.4	'gp4'	2.664520	2.758667
0.5	'gp5'	2.701723	2.794312
0.6	'gp6'	2.726334	2.819634
0.7	'gp7'	2.743927	2.837242
0.8	'gp8'	2.756226	2.849289
0.05	'g05'	1.211647	1.230606
0.10	'g10'	1.259331	1.278259
0.15	'g15'	1.285843	1.304749
0.20	'g20'	1.300919	1.319977
0.25	'g25'	1.310349	1.329392
0.30	'g30'	1.316086	1.334999
0.05	'g05'	1.075264	1.090897
0.10	'g10'	1.121864	1.137848
0.15	'g15'	1.147645	1.163574
0.20	'g20'	1.163193	1.179146
0.25	'g25'	1.172264	1.188179
0.30	'g30'	1.178024	1.193985
0.05	'g05'	0.959969	0.973572
0.10	'g10'	1.005066	1.018852
0.15	'g15'	1.030686	1.044350
0.20	'g20'	1.045738	1.059464
0.25	'g25'	1.055008	1.068817
0.30	'g30'	1.060890	1.074570

output data file for gap and parallel capacitance

Freq(GHz)	Gap/2	Cgap(fF)	Cpar(fF)
.3200E+11	.1000E–03	1.4789	55.8182
.3200E+11	.2000E–03	1.0326	45.8325
.3200E+11	.3000E–03	.8946	40.4891
.3200E+11	.4000E–03	.8200	37.3474
.3200E+11	.5000E–03	.7594	35.3625
.3200E+11	.6000E–03	.7176	34.0614
.3200E+11	.7000E–03	.6859	33.2005
.3200E+11	.8000E–03	.6594	32.6301
.3600E+11	.1000E–03	1.5487	60.9670
.3600E+11	.2000E–03	1.1390	48.8567
.3600E+11	.3000E–03	.9906	42.7917
.3600E+11	.4000E–03	.8371	39.3528
.3600E+11	.5000E–03	.7638	37.1171
.3600E+11	.6000E–03	.7307	35.6390
.3600E+11	.7000E–03	.7012	34.6583
.3600E+11	.8000E–03	.6784	34.0021
.4000E+11	.1000E–03	.9855	67.4308
.4000E+11	.2000E–03	.5812	53.0624
.4000E+11	.3000E–03	.4080	46.0020
.4000E+11	.4000E–03	.3403	41.8948
.4000E+11	.5000E–03	.2266	39.3973
.4000E+11	.6000E–03	.2156	37.7064
.4000E+11	.7000E–03	.1925	36.5680
.4000E+11	.8000E–03	.1688	35.8057
.8600E+11	.5000E–04	.1896	20.3573
.8600E+11	.1000E–03	.1417	16.8361
.8600E+11	.1500E–03	.1209	15.0875
.8600E+11	.2000E–03	.1154	14.1369
.8600E+11	.2500E–03	.1090	13.5670
.8600E+11	.3000E–03	.1017	13.2336
.9400E+11	.5000E–04	.1893	21.5289
.9400E+11	.1000E–03	.1504	17.6024
.9400E+11	.1500E–03	.1257	15.7299
.9400E+11	.2000E–03	.1148	14.6790
.9400E+11	.2500E–03	.1073	14.0[illegible]
.9400E+11	.3000E–03	.1050	13.7098
.1020E+12	.5000E–04	.2249	22.9300
.1020E+12	.1000E–03	.1667	18.5599
.1020E+12	.1500E–03	.1346	16.4805
.1020E+12	.2000E–03	.1236	15.3471
.1020E+12	.2500E–03	.1190	14.6777
.1020E+12	.3000E–03	.1101	14.2771

LIST OF REFERENCES

1. Tatsuo Itoh, *Analysis of Microstrip Resonators*, IEEE Trans. Microwave Theory and Techniques, vol. MTT–22, pp. 946–952 (1974).

2. Paul Mark Shayda, *Spectral Domain Analysis of Fin–line*, M.S.E.E. Thesis, Naval Postgraduate School, Monterey, California, December 1979.

3. Tatsuo Itoh, *Numerical Techniques for Microwave Passive Structures*, John Wiley & Sons, Chapter 5, 1989.

4. Roberto Sorrentino and Tatsuo Itoh, *Transverse Resonance Analysis of Finline Discontinuities*, IEEE Trans. Microwave Theory Tech., vol. MTT–32, pp. 1633–1638 (1984).

5. Aosheng Rong and Sifan Li, *Frequency–Dependent Characteristics of Gap discontinuities in Suspended Striplines for Millimeter Wave Applications*, IEEE MTTS Digest, pp. 355–358 (1988).

6. Y. Shu, Y. Qi, Y. Wang, *Analysis Equations for Suspended Substrate Microstrip line and Broadside–Coupled Stripline*, IEEE Microwave Theory Tech. Symposium Digest, pp. 693–696 (1987).

7. Tatsuo Itoh and R. Mittra, Spectral–Domain Approach for Calculating the Dispersion Characteristics of Microstrip Lines, IEEE Trans. Microwave Theory Tech. (Short paper), vol. MTT–21, pp. 496–499, July 1973.

8. Jae Soon Jeong, An Evaluation of Coplanar Line for Application in Microwave Integrated Circuitry, M.S.E.E. Thesis, Naval Postgraduate School, Monterey, California, December 1988.

INITIAL DISTRIBUTION LIST

		No. Copies
1.	Defense Technical Information Center Cameron Station Alexandria, VA 22304 – 6145	2
2.	Library, Code 0142 Naval Postgraduate School Monterey, CA 93943 – 5002	2
3.	Department Chairman, Code EC Department of Electrical and Computer Engineering Naval Postgraduate School Monterey, CA 93943 – 5002	1
4.	Prof. Harry A. Atwater, Code EC/An Department of Electrical and Computer Engineering Naval Postgraduate School Monterey, CA 93943 – 5002	1
5.	Prof. H. M. Lee, Code EC/Lh Department of Electrical and Computer Engineering Naval Postgraduate School Monterey, CA 93943 – 5002	1
6.	Library of the Naval Academy Anggok dong, Jinhae city, Gyungnam 602–00 Republic of Korea	1
7.	Choi, Man Soo 4dong 403ho Keokdong APT. Gyesan Dong Buk Gu, Inchun city Republic of Korea	2
8.	Lcdr Hwang, Jung Sub SMC 1209 Naval Postgraduate School Monterey, CA 93943	1